Performance Evaluation of an Improved Fully Stressed Design Evolution Strategy on Simultaneous Topology, Shape and Size Optimization of Large-Scale Truss Structures

Ali Ahrari[a*] and Kalyanmoy Deb

COIN Report Number 2016023

Notice

This is the pre-print version of the paper entitled "*An improved fully stressed design evolution strategy for layout optimization of truss structures*" published in "Computers & Structures". Some revisions were performed in the subsequent stages. Please use the published version [1] for citation. If you are interested in this work but do not have access to the published version, please contact the corresponding author.

[1] Ahrari, A., & Deb, K. (2016). An improved fully stressed design evolution strategy for layout optimization of truss structures. Computers & Structures, 164, 127-144. doi:10.1016/j.compstruc.2015.11.009

The **source code in MATLAB**, with some minor revisions, is also available at the Research Gate page of the first author:
https://www.researchgate.net/publication/296694688_Source_code_for_the_improved_fully_stressed_design_evolution_strategy_FSD-ES_II

Performance Evaluation of an Improved Fully Stressed Design Evolution Strategy on Simultaneous Topology, Shape and Size Optimization of Large-Scale Truss Structures

Ali Ahrari[a] and Kalyanmoy Deb[b]

[a] *Graduate Student. Department of Mechanical Engineering, Michigan State University, East Lansing, MI, USA, email: aliahrari1983@gmail.com*

[b] *Koenig Endowed Chair Professor, Department of Electrical and Computer Engineering, Michigan State University, East Lansing, MI, USA, email: kdeb@egr.msu.edu, http://www.egr.msu.edu/~kdeb*

Abstract During the recent decade, truss optimization by metaheuristics has gradually replaced deterministic and optimality criteria-based methods. While they may provide some advantages regarding their robustness and ability to avoid local minima, the required evaluation budget grows fast when the number of design variables is increased. This practically limits the size of the problems to which they can be applied. Furthermore, most recent stochastic optimization methods handle the size optimization only, the potential saving from which is highly limited, when compared to the most sophisticated, and obviously the most challenging scenario, simultaneous topology, shape and size (TSS) optimization. In a recent study by the authors, a method based on combination of optimality criteria and evolution strategies, called fully stressed design based on evolution strategies (FSD-ES), was proposed for TSS optimization of truss structures. FSD-ES outperformed available truss optimizers in the literature, both in efficiency and robustness. The contribution of this study is two-fold. First, an improved version of FSD-ES method, called FSD-ES-II, is proposed. In comparison with the earlier version, it takes the displacement constraints in the resizing step into account and can handle constraints governed by practically used specifications. Update of strategy parameters is also revised following contemporary and new developments in evolution strategies. Second, a test suite consisting of large scale TSS optimization problems is developed to overcome some shortcomings in available benchmark problems. For each problem, performance of FSD-ES-II is compared with the best results available in the literature, often showing a significant superiority.

Keywords: Covariance matrix self-adaptation, Mixed-variable problem, Structural optimization, Stochastic rounding, Adaptive penalty function

1 Introduction

Truss design optimization can be considered from three distinct perspectives. Topology optimization determines the optimum connection plot of members. Shape optimization optimize coordinates of the nodes for a known topology and size optimization finds the optimum cross sections of the members. The optimized structure should satisfy some constraints on member stress, node displacement, slenderness ratio or even natural frequency.

The methods commonly used for truss optimization are based on optimality criteria or mathematical programing [1, 2]. The former assumes that the optimal design should satisfy a priori conditions [3]. The concept of fully stressed design (FSD) is the most common approach in this group, which assumes in the optimally sized structure, all members reach the stress limit at least in one of the load cases [3]. Accordingly, all members are iteratively resized to reach this goal, assuming that the force distribution does not change when members are resized. This assumption is perfectly valid for determinate structures, in which FSD can potentially reach the global minimum in one iteration. This is not the case for indeterminate structures, however, when the number of redundant members is small, the error prompted by this assumption is usually small, and iterative resizing, at least when the resizing step is controlled [3], can reach a high quality design. The required number of design evaluations is almost independent of the number of members [3], and the method usually reaches a good solution after a few iterations [3]. Later, the concept of FSD was extended to handle problems with multiple load cases, displacement constraints, or when more sophisticated failure criteria are governed by design specifications [1].

For these reasons, FSD used to be preferred over mathematical programming, when the computation resources were limited [3], except for highly indeterminate structures, where FSD risks divergence [3]. However, it does not take the objective function into account and thus, use of more sophisticated objective functions that consider other factors in the overall cost, is not directly applicable. When there are multiple displacement constraints, FSD leads to a resizing problem which is not easy to solve analytically.

Unlike optimality criteria, mathematical programming are robust tools to solve general optimization problems [3]. With recent development in computation tools and parallel computing, the challenge of costly evaluations has been moderated to great extent. At the same time, stochastic optimization techniques such as evolutionary algorithms (EAs) and swarm-based methods were developed and demonstrated some advantages over deterministic approaches, especially in

multimodal problems. There has been a large number of studies on truss optimization with stochastic methods in the recent decade. Most of them, however, consider the simplest scenario, size optimization. The number of recent publications on size optimization with stochastic methods is relatively huge, too many to cite. Some examples can be found in [4, 5].

More sophisticated schemes consider shape or topology optimization as well. Topology optimization is particularly a challenging task, since even a small variation in topology can result in significant change in member forces and besides, many kinematically unstable structures might be produced during the search. The most sophisticated scheme, and potentially the most effective one [2], performs topology, shape and size (TSS) optimization at the same time. Nevertheless, studies on TSS optimization are comparatively scarce, possibly because of the complexity of the problem nature which demands sophisticated specialization of metaheuristics. Several strategies to circumvent this complexity, in the case of TSS optimization, were proposed in the literature, however, they usually reduces potential for better solutions [6]. Moreover, the size of the test problems employed to validate the algorithms is usually small or moderate at best [7, 8, 9, 10, 11]. A few studies tried fairly large problems as well [12, 13, 6], but comparison with other methods were not provided.

In a recent method, called fully stressed design based evolution strategy (FSD-ES) [14, 6], the concept of FSD was employed to resize the designs produced by an evolution strategy. In comparison with earlier stochastic optimization methods, FSD-ES could reach lighter structures in smaller number of function evaluations. The resizing step helps the method find near optimally sized structure for a given shape or topology defined by the evolution strategy.

This study aims at overcoming some general drawbacks in stochastic TSS truss optimization by improving the earlier version of FSD-ES. The contributions of this study to truss optimization field are as follows:

- An improved version of the resizing technique is proposed, which can take displacement constraints into account. We also propose an optimality criteria-based heuristic to solve the resizing problem.
- The employed evolution strategy is revised and the traditional mutative self-adaptation concept is replaced by a strategy based on contemporary evolution strategies.

- A revision to the fitness function is provided to compare kinematically unstable structures as well.
- Emphasis is put on large-scale TSS problems, with up to 308 design parameters. Some of the test problems are proposed in this study, by converting a simpler problem to a complicated TSS problem.

In the next section, previous work on two main components of FSD-ES are briefly reviewed. The improved method, called FSD-ES-II, is explained in section 3. A test suite consisting of large scale TSS truss optimization problems is formed in section 4 and results from FSD-ES-II are compared to the best available results in the literature in section 5.

2 Main parts

FSD-ES utilized two underlying concepts: The ES part performs the stochastic global search in the whole search space while the FSD part optimize the size variables of the solution provided by the ES. By using FSD, problem specific knowledge is incorporated to the algorithm. These two parts are briefly discussed in this section.

2.1 Fully Stressed Design (FSD)

In general, the truss optimization problem can be formulated as follows:

$$\begin{aligned}
&\text{Minimize } weight(\boldsymbol{\theta}) = \rho \sum_{i=1}^{N_m} A_i l_i \\
&\text{subject to} \\
&u_{kl} \le u_k^{\text{all}}, k = 1, 2, \dots, DN_n, l = 1, 2, \dots, N_l, \\
&|\sigma_{il}| \le \sigma_i^{\text{all}}, i = 1, 2, \dots, N_m, l = 1, 2, \dots, N_l, \\
&A_i \in \mathbb{A}, i = 1, 2, \dots, N_m,
\end{aligned} \tag{1}$$

where $\boldsymbol{\theta}$ determines a design. N_m, N_n and N_l are the number of members, nodes and load cases respectively. D=2 for planar and D=3 for spatial trusses. σ and u represent the member stress and the node displacement respectively and superscript 'all' stands for the allowable limit, which is known or can be computed. ρ_i, A_i and l_i are the density, cross-section area and length of the i-th member respectively and $\mathbb{A}$ is the given set of available sections.

FSD is based on iterative resizing of the member cross section areas to minimize the truss weight such that all constraints are satisfied. No change on the topology or shape is made and thus,

the only design parameters are member sections, $\boldsymbol{A}$. The force distribution is assumed to be independent of the member cross section areas. For this case, the effect of each member on displacement can be computed using the unit load method:

$$u_{kl}(\boldsymbol{A}) = \left| \sum_{i=1}^{m} \frac{c_{ikl}}{A_i} \right|, \qquad (2)$$

where c_{ikl}'s are known from the truss analysis. Since each displacement constraint depends on many or even all sections, solving the resizing problem, in general, is not easy. In a study [3], a two-step approach was employed such that in the first step, member sections are increased or decreased so that all stress constraints are satisfied and activated. In the second step, satisfaction of displacement constraints is pursued, while, no reduction in the cross section areas is allowed.

For the case with only one displacement constraint, using optimality criteria leads to [15]:

$$CE = \frac{\partial w}{\partial A_i} \Big/ \frac{\partial u}{\partial A_i}, i = 1,2, \dots, N_m, \qquad (3)$$

which can be interpreted as *cost effectiveness* (*CE*) of the *i*-th member in reduction of the constraint [15]. According to the equation 3, in the optimally sized structure, cost effectiveness of all members are the same. When sections are discrete, average cost effectiveness should be defined:

$$CE \cong \frac{\Delta w}{\Delta A_i} \Big/ \frac{\Delta g}{\Delta A_i}, i = 1,2, \dots, N_m, \qquad (4)$$

where ΔA_i is the difference between the current section area and the next/previous area in $\mathbb{A}$. For the more general case, when there are multiple displacement constraints, the common approach is to merge all displacement constraints into one constraint [15]. Schevenels et al. [15] proposed computation of average cost effectiveness of each member for all possible solutions around the current design, and selecting the one with the least average cost effectiveness. This process is repeated until a convergence condition is met. Although it was demonstrated that this strategy is able to reach a stable point, the computation of average cost effectiveness for all possible designs around the current design is exponentially expensive, which limits the number of independent sections in the problem.

2.2 Evolution strategies

Evolution strategies (ESs) are one the main streams of EAs which follow the principles of evolutionary biology including recombination, mutation and selection. In the general form, λ descendants are produced from μ parents. Selection is performed over the offspring only (comma

scheme) or the union of offspring and parents (plus scheme) to select parental population for the next generation. Mutation is rendered by variation of all variables simultaneously, using multivariate normal distribution. Parameters of the mutation distribution, called endogenous strategy parameters [16], are adjusted during the optimization. In traditional ESs, these parameters, are updated according to the concept of mutative self-adaptation [16] [17], according to which strategy parameters are mutated first, and the new solution is generated using the mutated parameters. Fitness of the individual is correlated to the aptness of the mutation and thus, strategy parameters are updated similar to the way the design (object) variables are.

In covariance matrix adaptation evolution strategy (CMA-ES) [18], known as the state of the art ES [19, 17], adaptation of the global step size is rendered using cumulation, and the covariance matrix is adapted in a de-randomized manner, in order to overcome some shortcomings of self-adaptation. For the same reasons, most contemporary evolution strategies employ the de-randomized approach [17].

CMA-ES, and its variants [17], provide spectacular results in unconstrained continuous parameter optimization, especially in ill-conditioned problems. Nevertheless, the complexity of the adaptation process reduces its flexibility, when applied to constrained mixed-variable problems. In another study [20], a simpler variant of this method, called CMSA-ES, was proposed which may compete with the original CMA-ES, at least when highly ill-conditioned problems are excluded. Because of its simplicity, it shows more flexibility for specialization for highly constrained mixed-variable TSS problems. The pseudo code of one iteration of CMSA-ES can be summarized as follows:

For j=1 to λ

$\sigma_j = \sigma_{\text{mean}} \exp\big(\tau \mathcal{N}(0,1)\big),\ \boldsymbol{z}_j = \sqrt{\mathbf{C}}\, \boldsymbol{\mathcal{N}}(\mathbf{0}, \mathbf{1}),\ \boldsymbol{x}_j = \boldsymbol{x}_{\text{mean}} + \sigma_j \boldsymbol{z}_j$

Compute $f(\boldsymbol{x}_j)$

End

Sort individuals ($\boldsymbol{x}_j$'s) based on their function value.

Let $\sigma_{\text{mean}} \leftarrow \prod_{j=1}^{\mu}\big((\sigma_j)^{w_j}\big)$, $\boldsymbol{x}_{\text{mean}} \leftarrow \sum_{j=1}^{\mu} w_j \boldsymbol{x}_j$, $\mathbf{C} \leftarrow \left(1 - \frac{1}{\tau_c}\right)\mathbf{C} + \frac{1}{\tau_c}\sum_{j=1}^{\mu} w_j \boldsymbol{z}_j \boldsymbol{z}_j^T$

In the pseudo code, λ is the population size, μ is the number of parents, σ_j is the individual step size generated from the global step size σ_{mean}, $\mathbf{C}$ is the covariance matrix and $\sigma_j \boldsymbol{z}_j$ is the perturbation applied to the recombinant design, $\boldsymbol{x}_{\text{mean}}$, to generate the new solution, $\boldsymbol{x}_j$. τ and τ_c are fixed numbers

specifying the learning rate for the global step size and the adaption interval for the covariance matrix respectively. w_j's specify the weights of parents in the updating process. In CMSA-ES, these weights are equal (w_j=1/μ), while in the original CMA-ES, logarithmically decreasing weights [18] ($w_j = (\ln(\mu+1) - \ln(j)) / \sum_{j=1}^{\mu}(\ln(\mu+1) - \ln(j))$) were preferred.

Several ES-based methods for structural optimization have been developed in the last decades [21, 22, 23]. However, most of them demonstrate significant deviation from the state-of-the-art ESs [14]. Although this might be necessary to handle mixed-variable highly constrained truss optimization problems, such modifications may result in a significant decline in capabilities of the method. Direct implementation of the standard CMA-ES for truss optimization, as performed in a few studies [24, 25], may have its own disadvantages. Size parameters should be assumed to be continuous, a condition which can hardly be met in practice. The CMA-ES method needs a separate handling of constraints, which remains a constant challenge to its users.

3. FSD-ES-II

The main steps of the FSD-ES-II are explained in details. Some steps are quite similar to the older version, FSD-ES [6].

3.1 Problem representation

In FSD-ES-II, each candidate design, $\boldsymbol{\theta}$, is represented by 3 vectors:

- $\boldsymbol{M}$ is a vector of size N_m, whose elements are Boolean variables that determine whether a member is active (M_i=1) or passive (M_i=0) in the design.
- $\boldsymbol{X}$ is a vector of size DN_n, whose elements are continuous variables that determine nodal coordinates, where D=2 for planar and D=3 for spatial trusses.
- $\boldsymbol{A}$ is a vector of size N_m, whose elements are discrete variables that determine member cross sections areas.

Accordingly, $\boldsymbol{\theta}$={$\boldsymbol{M}$, $\boldsymbol{X}$, $\boldsymbol{A}$} is a vector of size $2N_m+DN_n$, with upper and lower limits of $\boldsymbol{\theta}^u$ and $\boldsymbol{\theta}^l$ respectively.

3.2 ES-based sampling of new designs

Because of its simplicity, and thus flexibility for tailoring for highly constrained mixed-variable TSS problems, CMSA-ES is preferred over CMA-ES in this study. In FSD-ES-II, only diagonal

elements of the covariance matrix are considered. This reduces the covariance matrix to vector $\boldsymbol{d}$, which is of the size of $\boldsymbol{\theta}$. all solutions are sampled by applying a perturbation to the recombinant design, $\boldsymbol{\theta}_{\text{mean}}=\{\boldsymbol{M}_{\text{mean}}, \boldsymbol{X}_{\text{mean}}, \boldsymbol{A}_{\text{mean}}\}$. In the first iteration, $\boldsymbol{X}_{\text{mean}}$ and $\boldsymbol{A}_{\text{mean}}$ are the center of the range defined by the search space limits. $\boldsymbol{M}_{\text{mean}}=\mathbf{1}$ so that most sampled solutions in the early iterations have sufficient number of members. To generate a new solution, the global step size is mutated first:

$$\sigma_j = \sigma_{\text{mean}} \exp\big(\tau \mathcal{N}(0,1)\big). \tag{5}$$

σ_j is then used to generate $\boldsymbol{\theta}_j$:

$$\boldsymbol{\Theta}^{\text{up}} = \boldsymbol{F}\big(\boldsymbol{\theta}^{\text{U}}, \boldsymbol{\theta}_{\text{mean}}, \sigma_j \boldsymbol{d}\big), \boldsymbol{\Theta}^{\text{low}} = \boldsymbol{F}\big(\boldsymbol{\theta}^{\text{L}}, \boldsymbol{\theta}_{\text{mean}}, \sigma_j \boldsymbol{d}\big), \tag{6}$$

$$\boldsymbol{\theta}_j = \boldsymbol{F}^{-1}\big(\boldsymbol{r} \otimes \big(\boldsymbol{\Theta}^{\text{up}} - \boldsymbol{\Theta}^{\text{low}}\big) + \boldsymbol{\Theta}^{\text{low}}, \boldsymbol{\theta}_{\text{mean}}, \sigma_j \boldsymbol{d}\big), \tag{7}$$

where $\boldsymbol{F}(\boldsymbol{\theta}^{\text{U}}, \boldsymbol{\theta}_{\text{mean}}, \sigma_j \boldsymbol{d})$ computes the cumulative function of normal distribution at $\boldsymbol{\theta}^{\text{U}}$ with mean of $\boldsymbol{\theta}_{\text{mean}}$ and standard deviation of $\sigma_j \boldsymbol{d}$ in an element-wise manner. The sign $\otimes$ denotes element-wise multiplication and $\boldsymbol{r}$ is a vector of uniform random numbers in [0, 1]. Equation 6 demonstrates that $\boldsymbol{\theta}_j$ is sampled from the truncated normal distribution such that it falls within the limits defined by $\boldsymbol{\theta}^{\text{L}}$ and $\boldsymbol{\theta}^{\text{U}}$. $\boldsymbol{\theta}_j$ consists of continuous numbers and thus cannot be evaluated. The stochastic rounding technique utilized in FSD-ES [6] is applied to size and topology variables to create the actual design, which stochastically rounds the size and the topology variables to the upper or lower permissive value. The flowing necessary conditions are then checked for kinematic stability and acceptability of the generated design [26]:

- All necessary nodes must be active.
- Truss must have at least the minimum number of members required for kinematic stability: The number of active members plus the number of reactions from the supports must be equal or greater than the number of active nodes multiplied by D.
- The number of members connected to an active node plus the number of reactions on that node must be equal or greater than D.

Checking these necessary, but not sufficient, conditions for kinematic stability is computationally inexpensive, since it does not require performing a finite element analysis. If the generated design does not satisfy any of these conditions, it is discarded and a new topology is sampled. This process continues until a design that satisfies all these conditions is generated and accepted. For each accepted design, vector $\boldsymbol{\varpi}_j^X$ of size DN_{n} and vector $\boldsymbol{\varpi}_j^A$ of size N_m store the data

pertaining to activeness or passiveness of shape and size variables in $\boldsymbol{\theta}_j$ respectively. These vectors consists of Boolean variables, in which '1' refers to an active and '0' refers to a passive size or shape variable. These vectors are utilized to exclude the effect of passive shape and size variables on the updating process, which is explained in section 3.5.

3.3 Design evaluation

Analytically, a truss is kinematically stable if an only if the determinant of the stiffness matrix is not zero; however, since software computes the determinant numerically and the precision is limited, this cannot be employed as a reliable metric. In this study, the command '*rcond*' of MATLAB© software is used to calculate an estimate for the condition number of the stiffness matrix. It is assumed that truss is kinematically stable if and only if $rcond(\mathbf{K}_j)>10^{-12}$, where $\mathbf{K}_j$ is the stiffness matrix of the structure. If the truss is found to be kinematically unstable, the cost of the truss is assigned as follows:

$$f(\boldsymbol{\theta}_j) = 10^{100} \times \left(1 + \frac{nul(\mathbf{K}_j) + N_j^{\text{red}}}{N_j^{\text{req}}}\right), \quad \text{if} \quad rcond(\mathbf{K}_j) \leq 10^{-12}, \tag{8}$$

where $nul(\mathbf{K}_j)$ is nullity of $\mathbf{K}_j$, N_j^{req} is the minimum number of members required for kinematic stability of the truss and N_j^{red} is the number of redundant members. Applying the coefficient of 10^{100} ensures all kinematically unstable structures are inferior to all stable ones. $nul(\mathbf{K}_j)$ is an integer number which shows how much the structure is far from kinematic stability, or equivalently, how kinematically unstable the structure is. This provides a unique tool for comparing even kinematically unstable designs so that by preferring less kinematically unstable designs, the population size is directed towards regions with kinematically stable designs. Using equation (8) is and should be considered as a function evaluation, even though the full analysis of the structure is not performed, since it requires formation of the stiffness matrix and computation of the nullity, the required time for which is in the same order of a full analysis.

If the design is kinematically stable, the system response, including the member forces and node displacements to the external load(s), as well as the unit loads (required to compute c_{ikl}'s in Equation 2), are computed. FSD-ES [6] utilizes a specialized penalty function based on the estimated required increase in the cross section areas such that all constraints are satisfied. This required increase, when multiplied by the penalty coefficients, form the penalty term. The penalty term in FSD-ES-II follows the same strategy, with slight modification in formulation. First, for

each member, the smallest section area $\hat{A}_{ji} \geq A_{ji}$ is sought such that it satisfies all member-based constraints (slenderness, buckling and stress), assuming that the axial force does not change. If the largest section in $\mathbb{A}$ cannot satisfy these constraints, a virtual $\hat{A}_{ji}$ that satisfies these constraint is determined whose radius of gyration is equal to the radius of gyration of the largest section area in $\mathbb{A}$. $\hat{A}_{ji} - A_{ji}$ is the estimated required increase in the current value of A_{ji} so that the i-th member satisfies all member-based constraints. To compute the required increase for satisfaction of displacement constraints, section areas of all members are increased proportionally:

$$\check{A}_{ji} = A_{ji} \max_{k,l} \left\{ \left| \frac{u_{jkl}}{u_k^{\text{all}}} \right| \right\}, \qquad k = 1, 2, \dots, DN_n, l = 1, 2, \dots, N_l, \tag{9}$$

According to equation 9, if $\check{A}_{ji}$'s replace A_{ji}'s, all displacement constraints will be satisfied. The penalized objective function is calculated considering the estimated required increase in the structure weight as follows:

$$f(\boldsymbol{\theta}_j) = \sum_{i=1}^{N_m} \rho_i A_{ji} l_{ji} + \sum_{i=1}^{N_m} \rho_i l_{ji} \max\{P_i(\hat{A}_{ji} - A_{ji}), (\check{A}_{ji} - A_{ji})\}, \tag{10}$$

where $P_i \geq 1$ is the penalty coefficient for the i-th member, applied to member-based constraint violations only, since the required increase of $\hat{A}_{ji} - A_{ji}$ is computed assuming the member force does not change when the section is modified. If a displacement constraint is violated, all cross sections are proportionally increased, which does not affect member forces even in indeterminate structures, and thus, the penalty coefficients are not applied to the $\check{A}_{ji} - A_{ji}$ term. P_i's are iteratively adapted at the end of each iteration, as it will be explained in section 3.5. For the first iteration, $P_i = 1$, $i = 1, 2, \dots, N_m$.

3.4 Resizing

In the resizing step of FSD-ES, a new design ($\boldsymbol{\theta}_{j+\lambda}$) is generated by resizing the members of $\boldsymbol{\theta}_j$, without any change to the shape or topology variables. $\boldsymbol{\theta}_{j+\lambda}$ can be interpreted as a near optimally sized structure whose shape and topology is prescribed by $\boldsymbol{\theta}_j$. Member forces and coefficients c_{ijl}'s in Equation 2 are known from evaluation of $\boldsymbol{\theta}_j$, which are assumed to be independent of member cross section areas. Resizing is performed only if $\boldsymbol{\theta}_j$ is kinematically stable, otherwise we simply set $\boldsymbol{\theta}_{j+\lambda} = \boldsymbol{\theta}_j$. In FSD-ES-II, resizing is performed in two steps. In the first step, members are resized

for stress constraints and in the second step, the resized members are resized again so that all displacement constraints are satisfied.

3.4.1 Stress-based resizing

For each member, a new cross section is assigned such that the member satisfies all member-based constraints. Search for the acceptable section performs in a limited range around the current value:

$$\acute{A}_{ji}^{\mathrm{d}} = RoundUpA\left(\frac{A_{ji}}{1+(c_A-1)\exp(1-P_i)}\right), \acute{A}_{ji}^{\mathrm{u}} = RoundUpA\left(c_A A_{ji}\right),$$
$$\acute{A}_{ji} = FindAccSec\left([F_{i1}, F_{i2}, \dots, F_{iN_l}]; \acute{A}_{ji}^{\mathrm{d}}; \acute{A}_{ji}^{\mathrm{u}}\right), \quad (11)$$

where function *RoundUpA* rounds the argument to the nearest available section area in $\mathbb{A}$ and function *FindAccSec* finds the smallest acceptable section area ($\acute{A}_{ji}, \acute{A}_{ji}^{\mathrm{d}} \le \acute{A}_{ji} \le \acute{A}_{ji}^{\mathrm{u}}$) such that it satisfies all member-based constraints in all load cases. F_{il}'s are member forces in different load cases. If such a section cannot be found in the provided range, the function simply selects $\acute{A}_{ji} = A_{ji}^{\mathrm{u}}$. c_{A} controls the maximum possible change in $\acute{A}_{ji}$. As it will be explained in section 3.5, an increase in P_i implies in most recently generated solutions, $\acute{A}_{ji}$ has violated a constraint. If this happens, reduction of $\acute{A}_{ji}$ becomes more limited to prevent algorithm divergence. c_A is adapted iteratively based on the success of resizing in reduction of the cost, which will be explained in section 3.5. However, $c_A^{\mathrm{d}} \le c_A \le c_A^{\mathrm{u}}$, where c_A^{d} is the maximum of the ratio of areas of two successive sections in $\mathbb{A}$ and c_A^{u} is the ratio of the largest to the smallest areas in $\mathbb{A}$. For the first iteration, $c_A = c_A^{\mathrm{u}}$.

3.4.2 Displacement-based resizing

$\acute{A}_{ji}$'s determined from the stress-based resizing presumably satisfies all member constraints. However, the areas of some members should be increased to satisfy all displacement constraints as well. The complicated problem of finding out which member areas and how much to increase is handled by iteratively solving a very simple problem: At each iteration, the most critical displacement constraint (u_{c}) is selected and cost effectiveness of all members, when reduction of u_{c} is pursued, is computed. Combining Equations 2 and 3 leads to:

$$CE_{ji} = \left(\frac{\partial w}{\partial \acute{A}_{ji}} \Big/ \frac{\partial u_c}{\partial \acute{A}_{ji}}\right) = -\frac{\rho L \acute{A}_{ji}^2}{c_{jil}} \times \mathrm{sgn}\left(\sum_{i=1}^{m} \frac{c_{ikl}}{\acute{A}_{ji}}\right), i = 1,2,\dots,N_m, \quad (12)$$

The most efficient way to reduce u_0 is to increase the area of the section with minimum CE_{ji}. However, the value of CE_{ji} increases when the corresponding cross section area is increased, and

hence, the computed value of CE_{ji} should be updated whenever a small change is applied to $\acute{A}_{ji}$. Instead of finding the section with minimum CE_{ji} over and over, which is computationally expensive, a target cost effectiveness ($CE^{\mathrm{T}} \in [CE_0^{\mathrm{L}}, CE_0^{\mathrm{U}}]$) is found such that if all sections with $CE_{ji} < CE^{\mathrm{T}}$ are increased to have $CE_{ji} = CE^{\mathrm{T}}$, then u_{c} decreases by the desired amount:

$$\acute{u}_c = \max\left\{u_{\mathrm{c}}^{\mathrm{all}}, \frac{u_{\mathrm{c}}}{r_{\mathrm{uc}}}\right\}, \tag{13}$$

where $\acute{u}_{\mathrm{c}}$ is the goal value of u_{c} and $r_{\mathrm{uc}}>1$ specifics the desired reduction in u_{c}. Greater values of this parameter reduce the required computation by applying more change to member sections, however, the quality of the resized structure may reduce. By default, $r_{\mathrm{uc}}=1.05$. The search for CE^{T} is performed in the range

$$\left[CE_0^{\mathrm{L}}, CE_0^{\mathrm{U}}\right] = \left[\min_i\{CE_{ji}\}, \min\left\{100, 2^{10} \times \frac{u_{\mathrm{c}}}{\acute{u}_c}\right\} \times \min_i\{CE_{ji}\}\right], \tag{14}$$

using standard bisection method for 10 iterations, which computes CE^{T} with accuracy of r_{uc}^2. After finding CE^{T}, the new value of the sections to be changed are computed form Equation 12 as follows:

$$\acute{A}_{ji} \longleftarrow \begin{cases} \left|\dfrac{c_{jil} \times CE^T}{\rho_i l_i}\right|^{0.5}, & \text{if } CE_{ji} < CE^T, \\ \acute{A}_{ji}, & \text{otherwise.} \end{cases} \tag{15}$$

The structure with the new value of $\acute{A}_{ji}$ computed from Equation 15 reduces u_{c} to $\acute{u}_{\mathrm{c}}$, however, $\acute{A}_{ji}$'s are continuous values. The closest upper ($\acute{A}_{ji}^{+}$) and lower ($\acute{A}_{ji}^{-}$) section areas in $\mathbb{A}$ are found. Some $\acute{A}_{ji}$'s should be rounded to $\acute{A}_{ji}^{+}$'s to satisfy the desired change in u_{c}, while the rest should be rounded to $\acute{A}_{ji}^{-}$ to avoid unnecessary weight increase. The proper number (N_0) of sections to round to the upper values are sought so that in the resized design, u_{c} is reduced by the desired amount. These N_0 sections are selected based on their priority, which is the relative closeness to $\acute{A}_{ji}^{+}$:

$$\mathrm{Priority}\left(\acute{A}_{ji}\right) = \frac{\acute{A}_{ji} - \acute{A}_{ji}^{-}}{\acute{A}_{ji}^{+} - \acute{A}_{ji}^{-}}. \tag{16}$$

After rounding, $\acute{A}_{ji} \in \mathbb{A}$ and presumably $u_{\mathrm{c}} \leq \acute{u}_{\mathrm{c}}$. All u_{kl}'s are updated using Equation 2 when member sections are $\acute{A}_{ji}$. The most critical displacement constraint is detected again and reduced. This process continues until all displacement constraints are satisfied or the most critical displacement cannot be reduced anymore. The final $\acute{A}_{ji}$ specifies the sections of the new design:

$$A_{j+\lambda,i} = \acute{A}_{ji}, i = 1,2,\dots,N_m. \tag{17}$$

The new design is analyzed and evaluated using Equation 10.

3.5 Updating parameters

In addition to the strategy and design parameters of the evolution strategy, the penalty coefficients and the learning rates of $\boldsymbol{d}$ and σ_{mean} are updated at the end of each iteration.

3.5.1 Updating mutation parameters

The mutation parameters are the global step size, σ_{mean} and coordinate-wise scaling factors, $\boldsymbol{d}=[\boldsymbol{d}^{\text{M}}, \boldsymbol{d}^{\text{X}}, \boldsymbol{d}^{\text{A}}]$. All 2λ designs are sorted based on their objective function values. The best μ designs are selected to update σ_{mean} and $\boldsymbol{d}$. σ_{mean} is updated as follows:

$$\sigma_{\text{mean}} = \prod_{j=1}^{\mu}\left(\left(\sigma_j\right)^{w_j}\right), \tag{18}$$

which is very similar to the corresponding step in the original CMSA-ES [20], except that logarithmically decreasing weight (w_j's) [18] are used. $\boldsymbol{d}$ is updated as follows:

$$\boldsymbol{Z}_j^{\text{M}} \leftarrow \boldsymbol{M}^{\text{R}} - \boldsymbol{M}_j;\ \boldsymbol{Z}_j^{\text{X}} \leftarrow \boldsymbol{X}^{\text{R}} - \boldsymbol{X}_j;\ \boldsymbol{Z}_j^{\text{A}} \leftarrow \boldsymbol{A}^{\text{R}} - \boldsymbol{A}_j, j = 1,2,\dots,2\lambda,$$

$$\boldsymbol{d}^{X} \leftarrow \left(\left(1 - \frac{1}{\tau_c}\sum_{j=1}^{\mu} w_j \boldsymbol{\varpi}_j^{X}\right) \otimes \left(\boldsymbol{d}^{X} \otimes \boldsymbol{d}^{X}\right) + \frac{1}{\tau_c}\sum_{j=1}^{\mu} w_j \left(\boldsymbol{\varpi}_j^{X} \otimes \boldsymbol{Z}_j^{\text{X}} \otimes \boldsymbol{Z}_j^{\text{X}}\right)\right)^{0.5}, \tag{19}$$

$$\boldsymbol{d}^{\text{A}} \leftarrow \left(\left(1 - \frac{1}{\tau_c}\sum_{j=1}^{\mu} w_j \boldsymbol{\varpi}_j^{A}\right) \otimes \left(\boldsymbol{d}^{A} \otimes \boldsymbol{d}^{A}\right) + \frac{1}{\tau_c}\sum_{j=1}^{\mu} w_j \left(\boldsymbol{\varpi}_j^{A} \otimes \boldsymbol{Z}_j^{\text{A}} \otimes \boldsymbol{Z}_j^{\text{A}}\right)\right)^{0.5}. \tag{20}$$

In the sampling section, some topologies were discarded because of violation of a necessary condition. This rejection makes distribution of topology variables in the population anisotropic. To compensate this effect, in FSD-ES, adaptation of the topology variables and their corresponding scaling factors is based on comparison of values of topology variables in the offspring and parental populations:

$$\boldsymbol{d}^{\text{M}} \leftarrow \left(\boldsymbol{d}^{\text{M}} \otimes \boldsymbol{d}^{\text{M}} + \frac{1}{\tau_c}\left(\sum_{j=1}^{\mu} w_j \left(\boldsymbol{Z}_j^{\text{M}} \otimes \boldsymbol{Z}_j^{\text{M}}\right) - \frac{1}{2\lambda}\sum_{j=1}^{2\lambda}\left(\boldsymbol{Z}_j^{\text{M}} \otimes \boldsymbol{Z}_j^{\text{M}}\right)\right)\right)^{0.5}. \tag{21}$$

3.5.1 Updating the recombinant design

Shape and size variables of the recombinant design are updated by computing the weighted average of the parental population, however, the effects of passive members and nodes are excluded:

$$\boldsymbol{X}_{\text{mean}} \leftarrow \sum_{j=1}^{\mu} w_j \left(\left(\mathbf{1} - \boldsymbol{\varpi}_j^X \right) \otimes \boldsymbol{X}_{\text{mean}} + \boldsymbol{\varpi}_j^X \otimes \boldsymbol{X}_j \right), \tag{22}$$

$$\boldsymbol{A}_{\text{mean}} \leftarrow \sum_{j=1}^{\mu} w_j \left(\left(\mathbf{1} - \boldsymbol{\varpi}_j^A \right) \otimes \boldsymbol{A}_{\text{mean}} + \boldsymbol{\varpi}_j^A \otimes \boldsymbol{A}_j \right). \tag{23}$$

Because of anisotropy in distribution of topology variables, they are updated based on difference between their distribution in the offspring and parental populations. The proposed relation in FSD-ES-II is as follows:

$$\boldsymbol{M}_{\text{mean}} \leftarrow \boldsymbol{M}_{\text{mean}} + \left(\sum_{j=1}^{\mu} w_j \boldsymbol{M}_j - \frac{1}{2\lambda} \sum_{j=1}^{2\lambda} \boldsymbol{M}_j \right), \tag{24}$$

which is very similar to that of the FSD-ES. The new recombinant design is $\boldsymbol{\theta}_{\text{mean}}=\{\boldsymbol{M}_{\text{mean}}, \boldsymbol{X}_{\text{mean}}, \boldsymbol{A}_{\text{mean}}\}$.

3.5.3 Updating penalty coefficients

Adaptation of P_i's is performed based on the fraction of designs in the parental population in which the *i*-th member is responsible for a constraint violation. If this fraction is greater than 0.5, the corresponding penalty coefficient is increased. If a displacement constraint is violated, all members are assumed to be responsible for that. Accordingly, p_{ij} measures responsibility of the *i*-th member in possible constraint violation of the *j*-th design as follows:

- p_{ij}=0, if $\boldsymbol{\theta}_j$ is kinematically stable, the *i*-th member is active in the design, the design satisfies all displacement constraints and the *i*-th member does not violate a stress, slenderness or buckling constraint.
- p_{ij}=1, if $\boldsymbol{\theta}_j$ is kinematically stable, the *i*-th member is active in the design, but the design violates a displacement constraints or the *i*-th member violates a stress, slenderness or buckling constraint.
- p_{ij}=0.5, if $\boldsymbol{\theta}_j$ is kinematically unstable or the *i*-th member is passive in the design.

The value of 0.5 is a neutral value which neither increases nor decreases a penalty term. The weighted average of p_{ij}'s shows whether a penalty term should be increased or decreased:

$$\psi_i^{\text{old}} \leftarrow \psi_i^{\text{new}}, \qquad \psi_i^{\text{new}} \leftarrow \sum_{j=1}^{\mu} w_j \, p_{ji},$$

$$P_i \leftarrow \begin{cases} P_{i,} & \text{if } 0.5 < \psi_i^{\text{new}} < \psi_i^{\text{old}} \\ P_i \exp\left(\tau_P(\psi_i^{\text{new}} - 0.5)\right), & \text{otherwise.} \end{cases}, i = 1,2,\dots,N_m. \qquad (25)$$

where τ_P specifies the learning rate for the penalty coefficients. By default, $\tau_P=\tau^{0.5}$. $\psi_i^{\text{new}}>0.5$ refers that most of the times the i-th member has violated a constraint, and thus the corresponding penalty term should be intensified. It may take the algorithm several iterations to reach regions where $\psi_i^{\text{new}} < 0.5$. To give the algorithm the sufficient time, the corresponding penalty term is not intensified if $\psi_i^{\text{new}} < \psi_i^{\text{old}}$, which demonstrates some progress in moving towards the feasible regions was made.

3.5.4 Updating c_A

FSD assumes that the axial force remains constant when a cross section is changed. The error caused by this assumption increases when the amount of change increases, therefore, the resized solution might be even worse than the original one. The alternative is to reduce the possible amount of change in the section area, which is controlled by c_A, so that the error caused by the aforementioned assumption is reduced. The adaption of c_A is based on the resizing efficiency, which is proportional to the fraction of times in which the resized solution ($\boldsymbol{\theta}_{j+\lambda}$) is better than the original one ($\boldsymbol{\theta}_j$):

$$R_{\text{eff}} = \frac{1}{\lambda}\sum_{j=1}^{\lambda} \text{sgn}\left(1 - \frac{f\left(\boldsymbol{\theta}_{j+\lambda}\right)}{f\left(\boldsymbol{\theta}_j\right)}\right), \qquad c_A \leftarrow \max\left\{c_A^{\text{d}}, \min\left\{c_{\text{A}}^{\text{u}}, c_A \times \exp\left(R_{\text{eff}} \times \sqrt{\tau}\right)\right\}\right\}, \qquad (26)$$

where $-1 \le R_{\text{eff}} \le 1$ measures the resizing efficiency. Equation 26 indicates that c_{A} should increase if the resizing efficiency is high and vice versa.

3.6 Stopping criteria and parameter tuning

All parameters of the FSD part are set to their default values. In evolution strategies, τ, τ_{c}, μ and λ are selected based on the number of design parameters and population size for continuous unconstrained optimization. Our preliminary parameter study, in accordance with previous version

of FSD-ES [6], revealed that for highly constrained mixed-variable TSS optimization problems, the types of variables and the number of constraints should also be taken into account in computing the effective number design parameters. The proposed relation to compute the effective number of variables (N_{eff}) is as follows:

$$N_{\text{VAR}} = \left(\sqrt{N_{\text{top}}} + \sqrt{N_{\text{shape}}} + \sqrt{N_{\text{size}}}\right)^2, N_{\text{CON}} = \sqrt{N_l} \times \left(\sqrt{N_u} + \sqrt{N_m}\right)^2,$$

$$N_{\text{eff}} = (N_{\text{VAR}})\left(1 + \frac{N_{\text{CON}}}{N_{\text{VAR}}}\right)^{0.5}, \quad (27)$$

where N_{u} is the number of displacement constraints per load case and N_{top}, N_{shape} and N_{size} are the independent number of topology, shape and size variables. N_{VAR} is the effective number of design parameters and N_{CON} integrate the effect of the number of constraints. The parameters of the evolution strategy part are then set a follows:

$$\tau = \frac{1}{\sqrt{2N_{\text{eff}}}}, \tau_c = \frac{\mu + N_{\text{eff}} \times (N_{\text{eff}} + 1)}{\mu},$$

$$\lambda = 2\sqrt{N_{\text{eff}}}, \mu = [0.3\lambda], MaxIter = 75\sqrt{N_{\text{eff}}}. \quad (28)$$

The maximum number of iterations is set to a conservatively large value. However, based on the employed performance measure (section 5), the performance is measured by the consumed evaluation budget to reach the desired target weight instead of the allocated budget.

4 Test problems

To analyze and compare FSD-ES-II with the best TSS optimization methods, a test suite consisting of large-scale truss problems is formed. Simple test problems that are commonly employed in most available studies are overlooked. Some of the test problems are introduced in this study, mainly by converting an available shape and size optimization problem to a TSS optimization problem. Two goals are pursued by this modification: First, to measure the potential extra saving when a more flexible and intricate ground structure is used and second, whether employing an optimization method can detect such a potential gain, if any.

It is notable that some of the structures in the employed test problems are modular. For TSS optimization of modular trusses, the specialized formulation proposed in [27] can lead to better results than the conventional concept of the ground structure, nevertheless, in this study, the concept of the ground structure is employed for all problems in order to have a unified formulation

method. For clarity, only nodes are numbered in the ground structure, and members are determined by their end nodes. For example, $A_{1\text{-}2}$ denotes the cross section area of the member connecting node 1 to node 2.

4.1 47-bar transmission tower

The first problem is the 47-bar transmission tower truss problem, commonly employed as a shape and size optimization in many previous studies [27, 28, 29] but rarely as TSS optimization problem [28]. For shape and size optimization, FED-ES [14, 6] could reach a relatively lighter structure compared to available results in the literate. The TSS version of this problem is solved in this study by FSD-ES-II. Symmetry about x=0 is imposed which reduces the number of shape and size variables to 17 and 27 respectively. The search range for shape variables were not explicitly reported in [28], and thus a quite large range, with respect to the original configuration of the nodes in the depicted ground structure (Figure 1a) is considered in this study (Table 1). The ground structure has limited flexibility for topology optimization, since only 7 members ($A_{3\text{-}4}$, $A_{5\text{-}6}$, $A_{7\text{-}8}$, $A_{9\text{-}10}$, $A_{11\text{-}12}$, $A_{13\text{-}14}$, $A_{21\text{-}22}$) might be eliminated without kinematic instability of the structure, however, this information was not given to the method in [28]. For fair comparison, the same procedure is followed in this study and thus 27 topology variables are considered for this problem. Nodes 15, 16, 17 and 18 cannot move, and nodes 1 and 2 can move horizontally only.

Table 1. Simulation Data for the 47-bar truss problem

Design Variables	**Shape (17)**	$x_1, x_3, x_5, x_7, x_9, x_{11}, x_{13}, x_{19}, x_{21}, y_3, y_5, y_7, y_9, y_{11}, y_{13}, y_{19}, y_{21}$		
	Size (27)	27 size variables for 27 independent members, cross section of other members is dependent and determined using symmetry about x=0.		
	Topology (27)	One topology variable per size variable		
Constraints	**Stress**	$(\sigma_c)_i \le 103.42$ MPa (15 ksi); $(\sigma_c)_i \le 3.96EA_i/l_i^2$; $(\sigma_t)_i \le 137.90$ MPa (20 ksi), i=1, 2, …, 47		
	Displacement	None		
Search Range	**Shape Variables**	$-180'' \le x_1, x_3, x_5, x_7 \le -10''$; $-90'' \le x_9, x_{11}, x_{13}, x_{21} \le -10''$; $-150'' \le x_{19} \le -10''$; $120\times(i-1)'' \le y_{2i+1} \le 120\times(i+1)''$, i=1, 2, 3; $60\times(i+1)'' \le y_{2i+1} \le 60\times(i+3)''$, i=4, 5, 6; $560'' \le y_{19}, y_{21} \le 660''$;		
	Size Variables	$A \in \mathbb{A}$, $\mathbb{A}$ ={0.1, 0.2, 0.3, …, 4.9, 5} (in²)		
Loading		Nodes	F_x	F_y
	Case I	17,18	26.689 KN (6 kips)	-62.275 KN (-14 kips)
	Case II	17	26.689 KN (6 kips)	-62.275 KN (-14 kips)
	Case III	18	26.689 KN (6 kips)	-62.275 KN (-14 kips)
Mechanical Properties		Modulus of elasticity: E=206.84 GPa (3.0×10^4 ksi) Density of the material: ρ=8304.0 Kg/m³ (0.3 lb/in.^{3});		

1 in=2.54 cm, 1 in²= 6.452 cm²,

4.2 68-bar truss problem

The second test problem is TSS optimization of a 68-bar truss (Figure 1b) subjected to two load cases at the end, which is directly derived from [5]. Data required for simulation of this problem is presented in Table 2. Horizontal and vertical coordinates of the nodes may vary within 120″ and 40″ of the initial position in ground structure respectively. Nodes 1, 3, and 17 cannot be removed.

Table 2. Simulation data doe the 68-bar truss problem

Design Variables	**Shape (31)**	y_{17}, x_i, y_i, i=2,4,5,6,…, 14,15,16,18		
	Size (68)	a_i , i=1,2,…,68		
Constraints	**Stress**	$(\sigma_c)_i \leq$137.9 MPa (20 ksi); $(\sigma_t)_i \leq$137.9 MPa (20 ksi), $\lvert(\sigma_c)_i\rvert \leq \alpha E a_i / l_i^2$, i=1,2,…,68, α=3.96 i=1, 2, …, 68		
	Displacement	$u_j \leq$2.5 in., j=1, 2, 3, …, 68		
	Buckling			
Search Range	**Shape Variables**	Horizontal coordinates may vary within ±120 in of their initial value. Vertical coordinates may vary within ±40 in of their initial value.		
	Size Variables	$A_i \in$ **S** , i = 1, . . . , 68 **S**={0.111, 0.141, 0.174, 0.22, 0.27, 0.287, 0.347, 0.44, 0.539, 0.954, 1.081, 1.174, 1.333, 1.488, 1.764, 2.142, 2.697, 2.8, 3.131, 3.565, 3.813, 4.805, 5.952, 6.572, 7.192, 8.525, 9.3, 10.85} (in.^{2}) **S**={0.716, 0.910, …, 70.0} (cm^2)		
Loading		Nodes	F_x	F_y KN (kips)
	Case I	17	222.41 KN (-50 Kip)	0
	Case II	17	222.41 KN (-50 Kip)	-66.72 KN (-15 Kip)
	Mechanical Properties	Modulus of elasticity: E=206.84 GPa (3.0×10^4 ksi) Density of the material: ρ=0.081434 N/cm^3 (0.3 lb/in.^{3});		

4.3 77 bar bridge truss

This problem was adapted from [22], in which a bridge consisting of 20 panels with span of 20×300=6,000″ should carry a static uniform load applied to the lower cord (Figure 1c). The lower cord is pre-defined and cannot be modified. Such trusses are more realistic than those used in usual studies. In [22] several models were tried for the topology of the bridge, including Parker, K-truss and Pettit model, however, for each case, only the shape and the size were optimized while the topology remained fixed. Among them, the Parke model, when optimized, resulted in the lightest structure, and thus is selected to test FSD-ES-II on. Symmetry about x=3,000″ (center of the bridge) is exploited. Size variables are section area of the members on the left side of the symmetry plane and shape variables are vertical coordinates of the nodes on the upper cord. Data required for simulation of this problem are provided in Table 3.

Table 3. Simulation data for simulation of the 77-bar problem

Design Variables	**Shape (10)**	y_{2i+1}, i=1 2, …, 10		
	Size (39)	Cross sections of 39 members on the left side of the symmetry plane of the bridge, including those on the symmetry plane.		
	Topology (0)	No topology variable		
Constraints	**Stress**	AISC-ASD design specification, with F_y=248.21 MPa (36.0 ksi)		
	Displacement	$u_k \leq$ 25.4 cm (10″), k=1, 2,…, DN_n		
Search Range	**Shape Variables**	50″ $\leq y_{2i+1} \leq$ 1000″, i=1, 2, …, 10		
	Size Variables	$A \in \mathbb{A}$, where $\mathbb{A}$ is the set of 83 sections in W-shape profile list of AISC-ASD between W10×12 and W14×730.		
Loading		Node	F_x (kip)	F_y (kip)
		2, 4, 6, …, 38	0.0	−60.0
Mechanical Properties		Modulus of elasticity: E=200 GPa (29000 ksi)s Density of the material: ρ=7850 Kg/m^3 (0.2836 lb/in.^{3});		

4.4 110-bar transmission tower

The 47-bar transmission tower problem is revisited by proposing a more intricate ground structure to have more flexibility in the topology optimization phase. The alternative ground structure with 110-bar (Figure 2a) allows for elimination of redundant nodes as well. Nodes 21, 22, 23 and 24 cannot move and symmetry about x=0 is imposed. Presence of no member seems necessary for kinematic stability of the structure, and thus a topology variable per independent section is allotted, resulting in 60, 24 and 60 topology, shape and size variables respectively. Data required for simulation of this problem are provided in Table 4.

Table 4. Simulation Data for the 110-bar truss problem

Design Variables	**Shape (24)**	x_1, x_3, x_5, x_7, x_9, x_{11}, x_{13}, x_{15}, x_{17}, x_{19}, x_{25}, x_{27} y_3, y_5, y_7, y_9, y_{11}, y_{13}, y_{15}, y_{17}, y_{19}, y_{25}, y_{27}, y_{29}		
	Size (60)	60 size variables for 60 independent members, cross section of other members is dependent and determined using symmetry about x=0.		
	Topology (60)	One topology variable per size variable.		
Constraints (Variant I)	**Stress**	$(\sigma_c)_i \leq$103.42 MPa (15 ksi); $(\sigma_t)_i \leq$137.90 MPa (20 ksi), $(\sigma_c)_i \leq 3.96EA/l_i^2$		
	Displacement	No displacement constraint		
Search Range	**Shape Variables**	−180″ $\leq x_1, x_3, x_5, x_7, x_9 \leq$ 0″; −90″ $\leq x_{11}, x_{13}, x_{15}, x_{17}, x_{19}, x_{27} \leq$ 0″; −150″ $\leq x_{25} \leq$ 0″; 75×(i−1)″ $\leq y_{2i+1} \leq$ 75×(i+1)″, i=1, 2, 3, 4; 50×(i+1)″ $\leq y_{2i+1} \leq$ 50×(i+3)″, i=5, 6, 7, 8, 9; 550″ $\leq y_{25}, y_{27}, y_{29} \leq$ 650″;		
	Size Variables	$A \in \mathbb{A}$, $\mathbb{A}$ ={0.1, 0.2, 0.3, …, 4.9, 5} (in²)		
Loading		Nodes	F_x	F_y
	Case I	23, 24	26.689 KN (6 kips)	-62.275 KN (-14 kips)
	Case II	23	26.689 KN (6 kips)	-62.275 KN (-14 kips)
	Case III	24	26.689 KN (6 kips)	-62.275 KN (-14 kips)
Mechanical Properties		Modulus of elasticity: E=206.84 GPa (3.0×10^4 ksi);		
		Density of the material: ρ=8304.0 Kg/m³ (0.3 lb/in³);		

1 in=2.54 cm, 1 in²= 6.4516 cm²

Table 5. Simulation data for the 224-bar pyramid

sign Variables	**Shape (18)**	x_2, x_3, y_3, y_4, x_{18}, x_{19}, y_{19}, y_{20}, x_{34}, x_{35}, y_{35}, y_{36}, x_{50}, x_{51}, y_{51}, z_2, z_{18}, z_{34}			
	Size (32)	$A_{1\text{-}2}$, $A_{1\text{-}3}$, $A_{1\text{-}4}$, $A_{2\text{-}3}$ $A_{3\text{-}4}$, $A_{2\text{-}18}$, $A_{2\text{-}19}$, $A_{3\text{-}18}$, $A_{3\text{-}19}$, $A_{3\text{-}20}$, $A_{4\text{-}19}$, $A_{4\text{-}20}$, $A_{18\text{-}19}$, $A_{19\text{-}20}$, $A_{19\text{-}34}$, $A_{18\text{-}35}$, $A_{19\text{-}34}$, $A_{19\text{-}35}$, $A_{19\text{-}36}$, $A_{20\text{-}35}$, $A_{20\text{-}36}$, $A_{34\text{-}35}$, $A_{35\text{-}36}$, $A_{34\text{-}50}$, $A_{34\text{-}51}$, $A_{35\text{-}50}$, $A_{35\text{-}51}$, $A_{35\text{-}52}$, $A_{36\text{-}51}$, $A_{36\text{-}52}$, $A_{50\text{-}51}$, $A_{51\text{-}52}$			
	Topology (32)	One topology variable per size variable.			
Constraints	**Stress**	AISC-ASD design specification with F_y=248.21 MPa (36.0 ksi)			
	Displacement	$u_k \leq 1$ cm (0.39370″), k=1, 2,…, DN_n			
Search Range	**Shape Variables**	x_2, x_3, y_3, y_4 may vary within ±1.25 m of the default value in the ground structure. x_{18}, x_{19}, y_{19}, y_{20} may vary within ±2.5 m of the default value in the ground structure. x_{34}, x_{35}, y_{35}, y_{36} may vary within ±3.75 m of the default value in the ground structure. x_{50}, x_{51}, y_{51} may vary within ±5.0 m of the default value in the ground structure. z_2, z_{18}, z_{34} may vary within ±2.5 m of the default value in the ground structure.			
	Size Variables	$A \in \mathbb{A}$, where $\mathbb{A}$ is the set of circular hollow section in AISC-ASD			
Loading		Nodes	F_x (KN)	F_y (KN)	F_z (KN)
		1	500	500	−1000
Mechanical Properties		Modulus of elasticity: E=200 GPa (29000 ksi) Density of the material: ρ=7850 Kg/m³ (0.2836 lb/in³);			

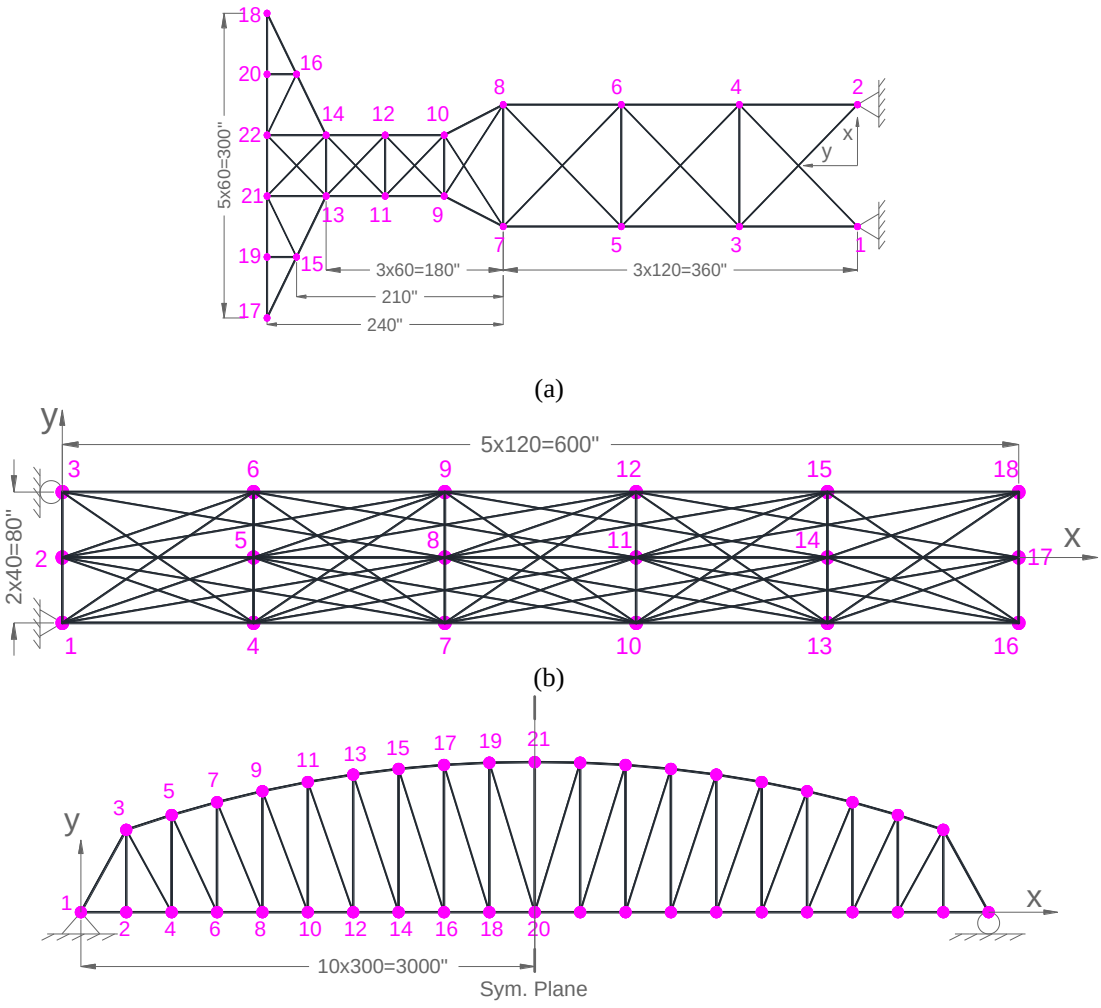


Figure 1. Ground structure for the a) 47-bar, b) 68-bar and c) 77-bar test problems.

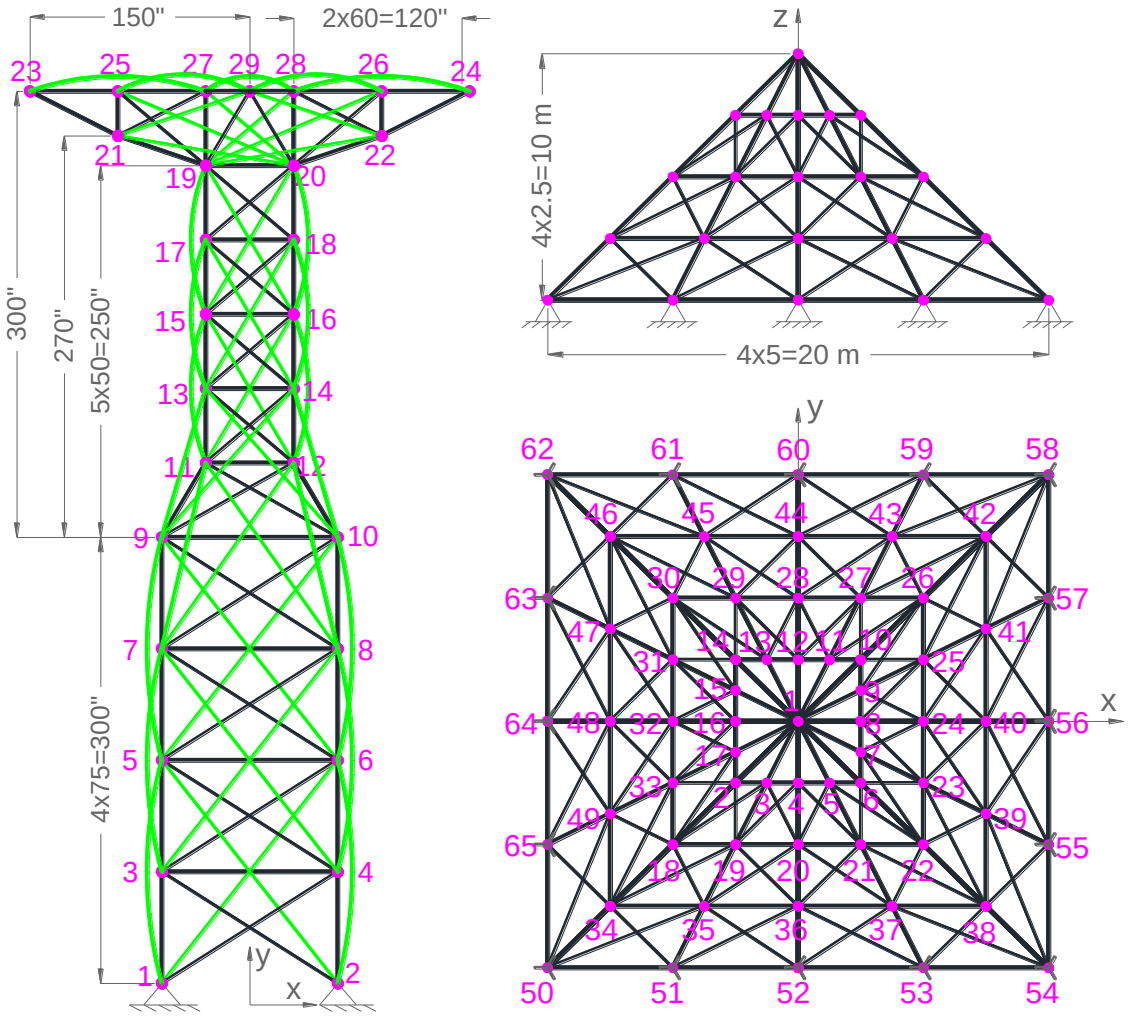


Figure 2. Ground structure for the a) 110-bar and b) 224-bar test problems

4.5 224-bar pyramid

The ground structure for the 224-bar pyramid test problem is depicted in Figure 2b, which is directly adopted from [12, 28]. There are 4 planes of symmetry (xy=0, $y\pm x$=0) and besides, for structural aesthetics, all nodes that have similar z in the ground structure must always have similar z. Nodes 1, 52, 56, 60 and 64 are critical nodes and cannot move in any direction. Other nodes, including the supports, can be eliminated if necessary. Despite the large number of members, the number of design variables is moderate. This problem has scarcely been used as a TSS optimization problem, despite the fact that it is more challenging and realistic than most conventional yet simple TSS problems. Design specifications are governed by AISC-ASD code. The search range of the shape variables and the material density were not explicitly mentioned in

the referenced studies, therefore, a relatively large range is selected in this study considering relative distance of nodes in the ground structure. The material density is set to 7,850 Kg/m³, a commonly used value for structural steel which also matches the results provided in [28]. Simulation data for this problem are provided in Table 5.

4.6 Bridge design problem

In the final step, the bridge design problem (77-bar truss problem) is revisited. Since there are many reasonable models for the topology, choosing the optimum one based on intuition is challenging, and besides, it is possible that the optimum topology of a panel depends on its location. For example, the Parker model may be the best choice for the 2nd panel, while the Pettit model might be the optimum choice for the 3rd one.

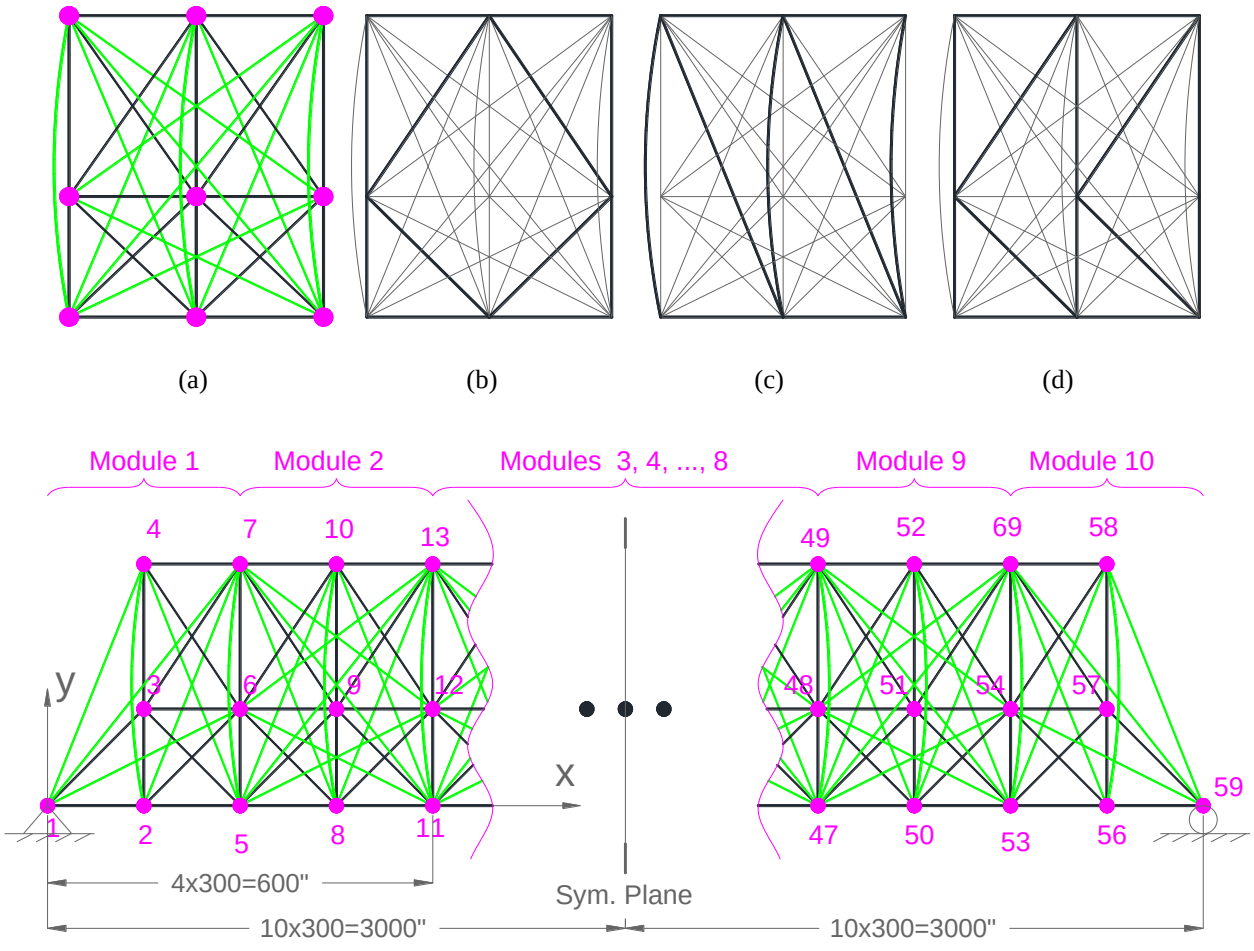


Figure 3. a) The proposed module for the bridge design problem. The proposed module can conform to different models such as b) Bailey c) Pratt and d) K-truss. e) The ground structure is posed by joining 10 of these modules side by side. For esthetics, some members of the first and the last modules were removed.

To reduce the burden on the designer for deciding on these important factors, this problem is revisited by proposing an intricate ground structure, consisting of 10 modules. Each module consists of 3×3=9 nodes and 33 members. The lower cord is pre-designed [22] and cannot be changed. Adjacent modules share 3 nodes and 3 members, thus the grounds structure has 59 nodes and 277 members. The selected module can conform to most models conventionally used for bridge design, including Parker, Bailey and K-truss, and many non-standard models. Three variants of this problem are solved in this study, with distinct amount of flexibility in the design.

- **Variant I**: The 1st and the 2nd modules are independent while modules 2, 3, 4 and 5 are topologically similar to the 2nd model. This reduces the number of topology parameters to 43. There is only one shape variable, vertical position of the upper cord. The height of nodes on the middle cord is half of the adjacent node on the upper cord. No node may move horizontally. There is one size variable per member on the left part of the bridge.
- **Variant II**: similar to variant I, but vertical position of the nodes on the upper cord are independent of each other, however, the height of nodes on the middle cord is half of the adjacent node on the upper cord, which increases the number of shape variable to 10.
- **Variant III:** Topologies of modules are independent of each other. There is one topology variable per member on the left part of the bridge except for the members on the lower cord, which must be active. Nodes on the middle and upper cord can move in any direction independent of each other, except the nodes on x=3,000″, which can move vertically only. The overall number of design variables is 308 for this case.

In all variants, symmetry about x=3,000″ is imposed, location of nodes on the lower cord is fixed and members on the lower cord (20 members) must remain active. Each variant provides more flexibility in design optimization than the previous one. This increases the potential material saving when optimization is performed, however, since the complexity of the problem exacerbates, the achieved solution might become even heavier than the previous variant, especially if the extra potential saving is small in comparison with the added complexity. Furthermore, modularity of the structure disrupts in later variants. For example, in variant I, shape and topology of modules are similar, which facilitates construction and improve esthetics. In variant II, modules are topologically similar, but differ in shape and cross sections. Finally, in variant III, the structure is not modular anymore. Whether the extra saving, if achieved, compensates for deterioration of structural esthetics and increase in construction costs depends on the amount of the saving, and is

a decision which should be made by the decision maker. Later variants are however more interesting for benchmarking, since they provide more challenging situations with larger number of design parameters, which can reliably illuminate the gap among different optimization methods.

The problem of possible overlapping members in the final design, which is assumed to be practically undesirable, is handled by imposing an overlap prevention rule: For a set of three nodes that must remain vertically aligned and are connected to one another (two short members and one long member), the long member may be active only if the two short members are passive. For example, this rule is applied to the set {2, 3, 4}. This means the long member can be active ($M_{2\text{-}4}$=1) only if the two short members are passive ($M_{2\text{-}3}$=$M_{3\text{-}4}$=0). A revision is performed to handle sampled designs that violate this rule. If a set of three members violates this rule, first a random number is generated ($r_0 \in [0, 1]$) and then, the following correction is applied:

$$\begin{cases} \text{Remove all 3 members,} & \text{if} \quad r_0 \le 0.2, \\ \text{Remove the long member,} & \text{if} \quad 0.2 \le r_0 \le 0.8, \\ \text{Remove the short members,} & \text{if} \quad 0.8 \le r_0. \end{cases}$$

The probabilities are computed based on the fact that in 8 possible combinations for absence/absence of 3 members, 5 combinations do not violate the overlapping rule. In 1 out of 5, no member is present, in 1 out of 5, only the long member is present and in 3 out of 5, at least one short member is present. This rule is applied to the 19 sets of vertically aligned nodes ({2, 3, 4}, {5, 6, 7}, …., {56, 57, 58}) in variants I and II. It is notable that this undesirable feature is unlikely to happen in variant III, since nodes may move horizontally as well. Data required for simulation of this problem are summarized in Table 6.

Table 6. Simulation data for the 277- bar bridge problem

Design Variables	**Shape**	**Variant I (1):** $y_4=y_7=\ldots=y_{58}=2y_3=2y_6=2y_9=\ldots=2y_{57}$ **Variant II (10):** $2y_{3i}=y_{3i+1}$, i=1, 2, …, 10 **Variant III (38):** x_{3i}, y_{3i}, x_{3i+1}, y_{3i+1}, i=1, 2, …, 9; y_{30}, y_{31}		
	Size	**All variants (140):** Cross sections of 140 members on the left side of the symmetry plane of the bridge, including those on the symmetry plane.		
	Topology	**Variants I & II (43):** $M_{1\text{-}3}$, $M_{1\text{-}4}$, $M_{1\text{-}6}$, $M_{1\text{-}7}$, $M_{2\text{-}3}$, $M_{2\text{-}4}$, $M_{2\text{-}6}$, $M_{2\text{-}7}$, $M_{3\text{-}4}$, $M_{3\text{-}5}$, $M_{3\text{-}6}$, $M_{3\text{-}7}$, $M_{4\text{-}5}$, $M_{4\text{-}6}$, $M_{4\text{-}7}$ (1st module) $M_{5\text{-}6}$, $M_{5\text{-}7}$, $M_{5\text{-}9}$, $M_{5\text{-}10}$, $M_{5\text{-}12}$, $M_{5\text{-}13}$, $M_{6\text{-}7}$, $M_{6\text{-}8}$, $M_{6\text{-}9}$, $M_{6\text{-}10}$, $M_{6\text{-}11}$, $M_{6\text{-}13}$, $M_{7\text{-}8}$, $M_{7\text{-}9}$, $M_{7\text{-}10}$, $M_{7\text{-}11}$, $M_{7\text{-}12}$, $M_{8\text{-}9}$, $M_{8\text{-}10}$, $M_{8\text{-}12}$, $M_{8\text{-}13}$, $M_{9\text{-}10}$, $M_{9\text{-}11}$, $M_{9\text{-}12}$, $M_{9\text{-}13}$, $M_{10\text{-}11}$, $M_{10\text{-}12}$, $M_{10\text{-}13}$ (2nd module) Apply overlap prevention rule		
		Variant III (130): One topology variable per member on the left side of the bridge except members on the lower cord.		
Constraints	**Stress**	AISC-ASD design specification, with F_y=248.21 MPa (36.0 ksi)		
	Displacement	$u_k \le 25.4$ cm (10″), k=1, 2,…, DN_n		
Search Range	**Shape Variables**	$50 \le y_{3i+1} \le 1000''$; i=1, 2, …, 10 $300''\times(i\text{-}1) \le x_{3i}$, $x_{3i+1} \le 300''\times(i+1)$, i=1, 2, …, 9		
	Size Variables	$A \in \mathbb{A}$, where $\mathbb{A}$ is the set of 83 sections in W-shape profile list of AISC-ASD between W10×12 and W14×730.		
Loading		Node	F_x (kip)	F_y (kip)

	2, 5, 8, …, 56	0.0	−60.0
Mechanical Properties	Modulus of elasticity: E=200 GPa (29000 ksi) Density of the material: ρ=7850 Kg/m^3 (0.2836 lb/in.^{3});		

5 Results and discussions

FSD-ES-II is employed to solve the employed optimization problems. All parameters are set to their default values, and thus the required tuning effort is zero. Each problem is solved 100 times independently and the best solution found is reported. However, comparing different methods solely based on the best solution found, as followed in most previous studies, is not a reliable method, due to stochastic nature of the experiment and possibility of obtaining better solutions if the evaluation budget or the number of independent runs is increased. The recommended performance measure is comparison of the expected running time (ERT) [30] to reach an arbitrary target weight (W_{target}).

$$ERT(W_{\text{target}}) = \frac{FEs(W_{\text{target}})}{SR(W_{\text{target}})}, \tag{29}$$

where $FEs(W_{\text{target}})$ is the average number of the require function evaluations to reach the desired target weight of W_{target}, provided that the run could reach W_{target}. SR is the fraction of runs in which the algorithm could reach W_{target}. FEs, SR and consequently ERT depends on W_{target}, and thus for each problem, these measures are plotted for a range of W_{target}. Unless only a few runs could reach W_{target}, these measures are robust with respect to stochastic nature the experiment. ERT is of particular interest, since it facilitates comparison of optimization methods by combining the effects of efficiency, measured by FEs, and reliability, measured by SR.

To increase reliability of statistical measures, each problem is solved 500 times independently. Because of the large number of independent runs, measured values of SR, FEs and ERT are assumed to be reliable if $SR \geq 0.05$. Figures 3 illustrate FEs, SR and ERT curves as a function of W_{target} for each problem. The best solution found for each problem is illustrated in Figures 4 and the corresponding design parameters are provided in Appendix. The obtained results demonstrate that:

- For the 47-bar truss problem, the best solution found by FSD-ES-II weighs 1,728 lb, reached after about 61,000 evaluations, although ERT is much greater. For W_{target}=1,750 lb, FEs=38,800 and SR=0.24, sufficiently high to draw reliable conclusions. In comparison with a previous GA-based method [28], which reached the best solution of 1,885 lb, at the

end of 100,000 evaluations, FSD-ES-II could reach an *8.3%* lighter structure relatively faster. For the case in which only shape and size optimization are performed, this problem has been solved with different methods in previous studies, among which the results provided by the earlier version of FSD-ES [6] outperformed the others. In comparison with the best design for shape and size optimization which weighs 1,847 lb [6], performing TSS optimization resulted in an extra *6.4%* reduction in the overall weight, which is quite significant considering the limited flexibility of the topology of the ground structure.

- For the 68-bar problem, the best solution of FSD-ES-II weighs 1,166 lb, about *3.1%* lighter than that found by FSD-ES [6]. More important, FSD-ES-II is several times faster when *ERT* of both methods are compared. Considering that some displacement constraints are active in the optimized solution, this advantage probably originates from the performed improvement in the resizing step so that the resizing scheme explicitly takes the displacement constraints into account.
- For the 77-bar bridge design problem, the best solution of FSD-ES-II weighs 306.0 kip, almost the same as the best solution of the earlier version [14]. The *FEs* of the older version is slightly smaller initially, however, for $W_{\text{target}} \leq 312$ kip, performance of both methods is similar. For this problem, best solution of Hasançebi [22] weighs W_{target}=317.1 kip, reached after about 150,000 evaluations. For the same target weight, FSD-ES-II is almost 8.5 times faster. The ground structure of this problem is determinate, where the assumption of FSD part are totally valid, which maximizes benefits of FSD concept. This could be one of the reasons for spectacular advantage of FSD-ES and FSD-ES-II over the ES-based method proposed in [22].
- For the 110-bar problem, the best solution of FSD-ES weighs 1,314 lb, which demonstrates by providing more flexibility in topology optimization, it is possible to save an extra *24%* in weight, when compared to the best solution of the 47-bar problem. The topology of the optimized solution could hardly be concluded by engineering intuition, even though it is only a little more complicated than the optimized solution of 47-bar problem. 28.6% of runs could reach W_{target}=1,450 lb, on average after 66,200 evaluations.
- For the 224 bar pyramid problem, the best solutions in the literature weighs 4,587 Kg [12], reached by an SA-based algorithm after 300 cooling cycles (presumably 24,600 function evaluations). The best solution of FSD-ES weighs 3,079 Kg, which is *32.8%* lighter than

the best reported solution in the literature. The required number of function evaluations for the best run to reach this weight is 113,000, relatively greater than the SA-based method, however, the gap between the qualities of the best designs is huge. Moreover, FSD-ES is a quasi-parameter free method, while in the SA-based method several parameters were tuned for the problem. For W_{target}=3,400 lb, *FEs*=87,400 and *SR*=0.17.

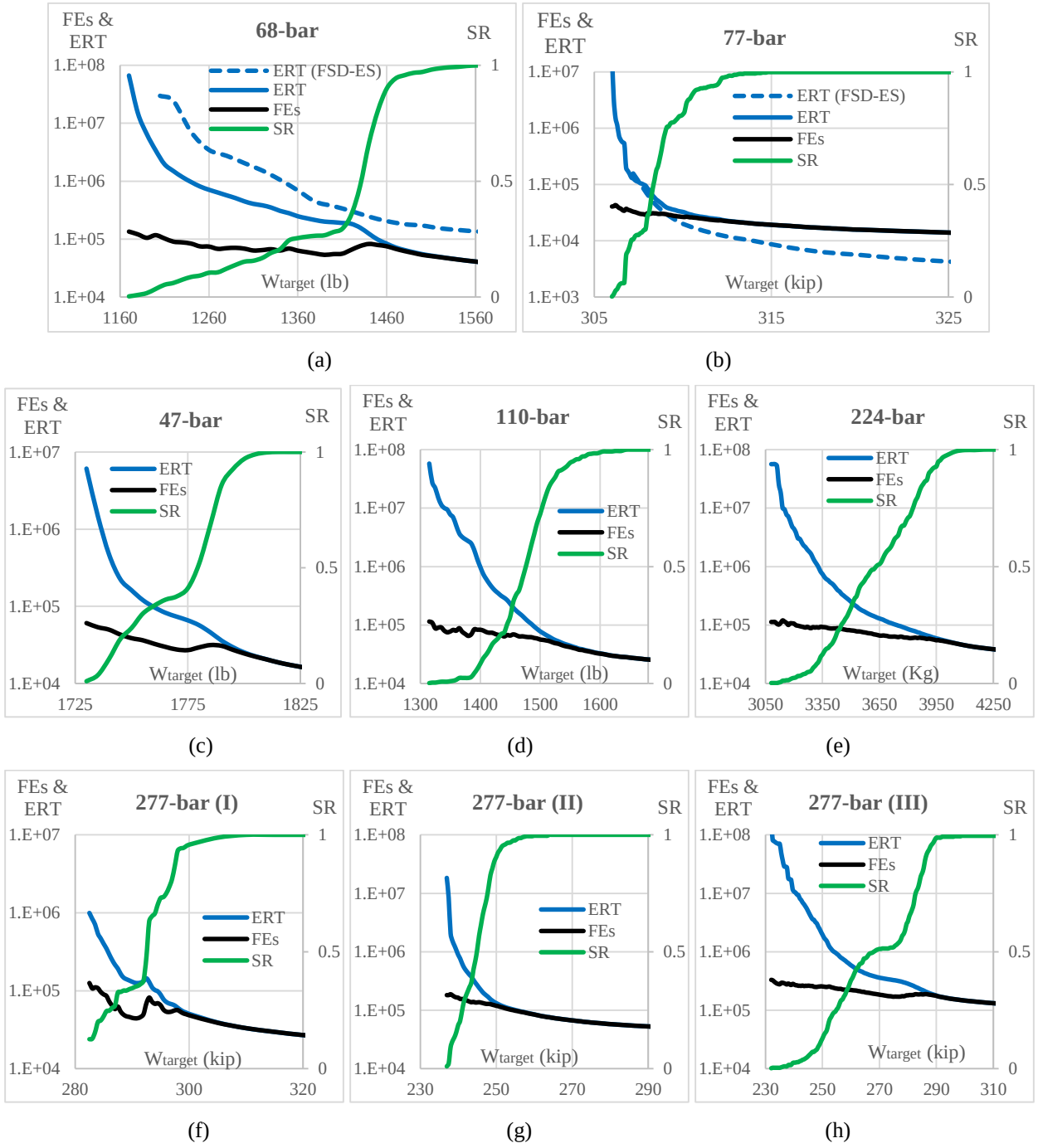


Figure 4. *FEs*, *SR* and *ERT* as a function of the target weight (W_{target}) for a) 68-bar, b)77-bar, c) 47-bar, d) 110-bar, e) 224-bar, f) 277-bar (Variant I), g) 277-bar (Variant II) and h) 277-bar (Variant III) test problems.

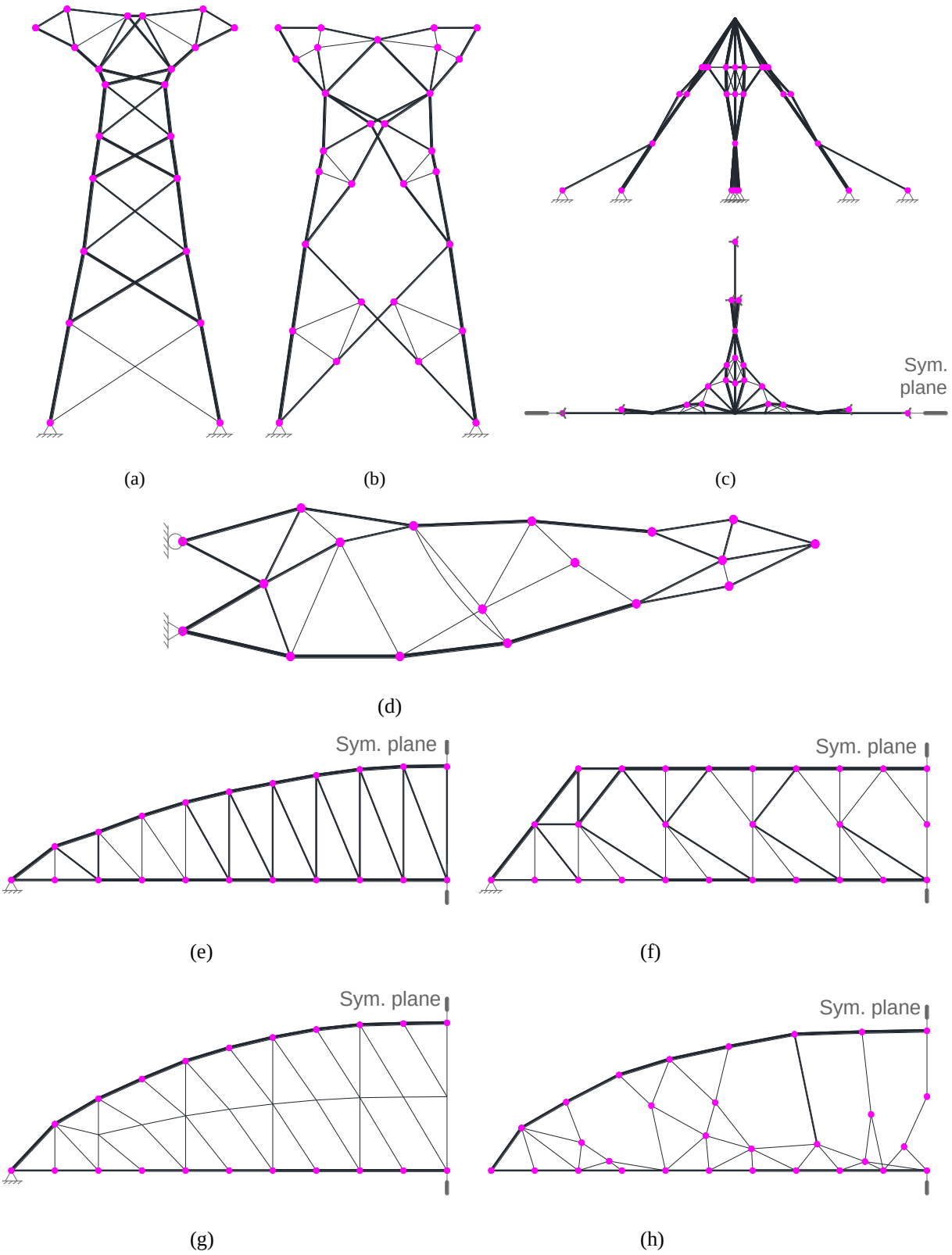


Figure 5. The best feasible solution found for diffeent test problems. a) 47-bar (W=1727.6 lb), b) 110-bar (W=1314.0 lb), c) 224-bar (W=3079.4 Kg), d) 68-bar (W=1166.1 lb), e) 77-bar (W=305.96 kip), f) 277-bar in case I (W=282.03 kip), g) 277-bar in case II (W=236.54 kip), h) 277-bar in case III (W=231.94 kip)

- In the variant I of bridge design problem, FSD-ES-II could reach the weight of 282.0 kip, which is surprisingly lighter than the best solution found in [22], even those that have higher flexibility for shape variation (317 kip [22], 307 kip [14] and 306 kip in the 77-bar test problem of this study). This demonstrates the optimized design of variant I is not only lighter, but also has less fabrication and assembly cost, due to similarity of modules (identical shape and topology versus identical topology only). It also excels in esthetics. The topology of the best solution found resembles the Bailey model to some extent. 12.6% of runs could each W_{target}=282.5 kip after 125,700 evaluations. The best solution of variant II of this problem weighs 236.5 kip, *16.1%* lighter than best solution of variant I and *22.7%* lighter than the case when the Parker model is optimized for shape and size. The arch-shape of the upper cord in the best found solution of variant II matches engineering intuition. In variant III, there is only *1.9%* achieved extra saving, in comparison with the best solution of variant II, which also comes at the cost of excessive function evaluations. For example, for W_{target}=240 kip, *ERT* in case III is about 12 times greater than the *ERT* in case II. The structural esthetics and ease of assembly has degraded as well.

6. Summary and conclusions

In this study, an improved version of the fully stressed design based on evolution strategy (FSD-ES) has been developed for simultaneous topology, shape and size (TSS) optimization of large-scale truss structures. In comparison with the earlier version, the new method, called FSD-ES-II, is able to explicitly handle displacement constraints in the resizing step. Some specialization on the evolution strategy part has also been performed to handle mixed variable nature of the TSS optimization problems while principles of the contemporary evolution strategies have been followed.

Efficiency and efficacy of the proposed FSD-ES-II have been tested on some complicated and large-scale TSS test problems to evaluate the algorithm for more practical and challenging scenarios. Three of the test problems, the 47-bar transmission tower, the 77-bar bridge and the 224-bar pyramid, have been directly adapted from the literature, for which FSD-ES-II could surpass the best available results by a clear margin. A few other test problems have been posed by converting available size and shape optimization problems to suitable TSS problems by providing more intricacy and flexibility in the ground structure. The results from FSD-ES-II on the newly

developed TSS problems have revealed that a huge saving (as high as 32%) in the structural weight can be achieved by more reliance on a potent optimization tool than human intuition. This highlights advantages of the computer methods in truss optimization field, where more reliance on optimization methods can result in superior results. Engineering intuition can be very helpful by defining a reasonable ground structure or problem formulation, to avoid unnecessary complexities.

Overall, the proposed FSD-ES-II has been demonstrated to handle a large number of design parameters, much larger than those usually considered in existing truss optimization studies, within a relatively small evaluation budget. More importantly, no ad-hoc parameter tuning is required with the proposed approach, thereby making FSD-ES-II a pragmatic tool for structural engineers.

The amount of saving in computation and the significant difference in performance compared to other contemporary methods in these problems have demonstrated a need for further research along the lines of our proposed algorithm. Realistic and complex TSS problems, including those developed in this study, may provide a reliable tool to compare different truss optimization methods in more realistic situations. It is believed that the introduction of these large-scale truss-structure optimization problems and their optimized solutions reported in this paper should remain as benchmark problems for future researchers in the area. After many decades of research, it is now time to demonstrate the power of current optimization methodologies to solve realistic problems so that the use of optimization can finally become a regular event in everyday design activities.

7. Acknowledgement

Computational work in support of this research was performed at Michigan State University's High Performance Computing Facility.

References

[1] M. P. Saka, "Optimum design of pin-jointed steel structures with practical applications," Journal of Structural Engineering, vol. 116, no. 10, pp. 2599-2620, 1990.

[2] B. H. V. Topping, "Shape optimization of skeletal structures: a review," Journal of Structural Engineering, vol. 109, no. 8, pp. 1933-1951, 1983.

[3] C. Feury and M. Geradin, "Optimality criteria and mathematical programming in structural weight optimization," Computers & Structures, vol. 8, no. 1, pp. 7-17, 1978.

[4] O. Hasançebi, S. D. E. Çarbaş, F. Erdal and M. P. Saka, "Performance evaluation of metaheuristic search techniques in the optimum design of real size pin jointed structures," Computers & Structures, vol. 87, no. 5, pp. 284-302, 2009.

[5] A. Kaveh and Z. A, "Comparison of nine meta-heuristic algorithms for optimal design of truss structures with frequency constraints," Advances in Engineering Software, vol. 76, pp. 9-30, 2014.

[6] A. Ahrari, A. A. Atai and K. Deb, "Simultaneous topology, shape and size optimization of truss structures by fully stressed design based on evolution strategy," Engineering Optimization, p. in press, 2014.

[7] K. Deb and S. Gulati, "Design of truss-structures for minimum weight using genetic algorithms," Finite elements in analysis and design, vol. 37, no. 5, pp. 447-465, 2001.
[8] H. Rahami, A. Kaveh and Y. Gholipour, "Sizing, geometry and topology optimization of trusses via force method and genetic algorithm," 2008, vol. 30, no. 9, pp. 2360-2369, Engineering Structures.
[9] G. C. Luh and C. Y. Lin, "Optimal design of truss-structures using particle swarm optimization," Computers & Structures, vol. 89, no. 23, pp. 2221-2232, 2011.
[10] L. F. F. Miguel, R. H. Lopez and L. F. F. Miguel, "Multimodal size, shape, and topology optimisation of truss structures using the Firefly algorithm. ,," Advances in Engineering Software, vol. 56, pp. 23-37, 2013.
[11] S. Gholizadeh, "Layout optimization of truss structures by hybridizing cellular automata and particle swarm optimization," Computers & Structures, vol. 125, pp. 86-99, 2013.
[12] O. Hasançebi and F. Erbatur, "Layout optimisation of trusses using simulated annealing," Advances in Engineering Software, vol. 33, no. 7, pp. 681-696, 2002.
[13] N. Noilublao and S. Bureerat, "Simultaneous topology, shape and sizing optimisation of a three-dimensional slender truss tower using multiobjective evolutionary algorithms," Computers & Structures,, vol. 89, no. 23, pp. 2531-2538, 2001.
[14] A. Ahrari and A. A. Atai, "Fully Stressed Design Evolution Strategy for Shape and Size Optimization of Truss Structures," Computers & Structures, vol. 123, pp. 58-67, 2013.
[15] M. Schevenels, S. McGinn, A. Rolvink and J. Coenders, "An optimality criteria based method for discrete design optimization taking into account buildability constraints," Structural and Multidisciplinary Optimization, p. in press, 2014.
[16] H. G. Beyer and H. P. Schwefel, "Evolution strategies–A comprehensive introduction," Natural computing, vol. 1, no. 1, pp. 3-52, 2002.
[17] T. Bäck, C. Foussette and P. Krause, Contemporary Evolution Strategies, Springer, 2013.
[18] N. Hansen and A. Ostermeier, "Completely derandomized self-adaptation in evolution strategies," Evolutionary computation, vol. 9, no. 2, pp. 159-195, 2001.
[19] O. Kramer, "Evolutionary self-adaptation: a survey of operators and strategy parameters," Evolutionary Intelligence, vol. 3, no. 2, pp. 51-65, 2010.
[20] H. G. Beyer and B. Sendhoff, "Covariance matrix adaptation revisited–the CMSA evolution strategy," in Parallel Problem Solving from Nature–PPSN X , Berlin Heidelberg, Springer, 2008, pp. 123-132.
[21] S. D. Rajan, "Sizing, shape, and topology design optimization of trusses using genetic algorithm," Journal of Structural Engineering, vol. 121, no. 10, pp. 1480-1487, 1995.
[22] O. Hasançebi, "Adaptive evolution strategies in structural optimization: Enhancing their computational performance with applications to large-scale structures," Computers & structures, vol. 86, no. 1, pp. 119-132, 2008.
[23] C. Ebenau, J. Rottschäfer and G. Thierauf, "An advanced evolutionary strategy with an adaptive penalty function for mixed-discrete structural optimisation," Advances in Engineering Software, vol. 36, no. 1, pp. 29-38, 2005.
[24] A. Kaveh, M. Kalateh-Ahani and M. S. Masoudi, "The CMA evolution strategy based size optimization of truss structures," International journal of optimization in civil engineering, vol. 2, pp. 233-256, 2011.
[25] W. Hare, J. Nutini and S. Tesfamariam, "A survey of non-gradient optimization methods in structural engineering," Advances in Engineering Software, vol. 59, pp. 19-28, 2013.
[26] D. Li, S. Chen and H. Huang, "Improved genetic algorithm with two-level approximation for truss topology optimization," Structural and Multidisciplinary Optimization, vol. 49, no. 5, pp. 795-814, 2014.
[27] A. Ahrari and A. Atai, "Efficient simulation for optimization of topology, shape and size of modular truss structures," International Journal of Optimization in Civil Engineering, vol. 3, no. 2, pp. 209-223, 2013.
[28] O. Hasançebi and F. Erbatur, "Layout optimization of trusses using improved GA methodologies," Acta mechanica, vol. 146, no. 1-2, pp. 87-107, 2001.
[29] E. Salajegheh and G. N. Vanderplaats, "Optimum design of trusses with discrete sizing and shape variables," Structural Optimization, vol. 6, no. 2, pp. 79-85, 1993.
[30] N. Hansen, A. Auger, S. Finck and R. Ros, "Real-Parameter Black-Box Optimization Benchmarking 2010: Experimental Setup," INRIA, 2010.
[31] C. Fleury, "An efficient optimality criteria approach to the minimum weight design of elastic structures," Computers & Structures, vol. 11, no. 3, pp. 163-173, 1980.
[32] S. R. Hansen and G. N. Vanderplaats, "Approximation method for configuration optimization of trusses," AIAA journal, vol. 28, no. 1, pp. 161-168, 1990.
[33] American Institute of Steel Construction (AISC). Manual of Steel Construction: Allowable Stress Design, 1989.
[34] O. Hasançebi, "Optimization of truss bridges within a specified design domain using evolution strategies," Engineering Optimization, vol. 39, no. 6, pp. 737-756, 2007.
[35] P. Hajela and E. Lee, "Genetic algorithms in truss topological optimization," International journal of solids and structures, vol. 32, no. 22, pp. 3341-3357, 1995.
[36] S. M. Shrestha and J. Ghaboussi, "Evolution of optimum structural shapes using genetic algorithm," Journal of Structural Engineering, vol. 124, no. 11, pp. 1331-1338, 1998.

Appendix: Parameters of the best solution found for each problem

47-bar		y_{15}	412.900	x_{12}	331.501	x_{36}	-478.008	$A_{14\text{-}16}$	55.8	$A_{24\text{-}29}$	14.4	$A_{20\text{-}23}$	39.9	$A_{1\text{-}2}$	19.1
(1727.6241 lb)		x_{17}	-10.813	y_{12}	58.396	y_{51}	-17.302	$A_{15\text{-}16}$	15.8	$A_{25\text{-}28}$	75.6	$A_{21\text{-}23}$	9.71	$A_{1\text{-}3}$	50
in & in^2		y_{17}	453.908	x_{13}	430.570	x_{51}	-657.798	$A_{15\text{-}17}$	75.6	$A_{26\text{-}29}$	55.8	$A_{21\text{-}24}$	6.49	$A_{2\text{-}3}$	6.49
x_1	-127.426	x_{19}	-78.574	y_{13}	-15.651	$A_{36\text{-}51}$	35.9999	$A_{16\text{-}17}$	14.4	$A_{28\text{-}30}$	9.71	$A_{22\text{-}24}$	9.71	$A_{2\text{-}5}$	20
x_3	-98.277	y_{19}	500.112	x_{14}	512.163	$A_{36\text{-}52}$	6.9032	$A_{16\text{-}18}$	55.8	$A_{28\text{-}31}$	75.6	$A_{22\text{-}25}$	56.8	$A_{3\text{-}4}$	55.8
y_3	151.332	x_{25}	-122.764	y_{14}	23.357	$A_{19\text{-}36}$	27.7419	$A_{17\text{-}18}$	21.8	$A_{29\text{-}30}$	6.49	$A_{23\text{-}24}$	9.71	$A_{3\text{-}5}$	9.71
x_5	-76.494	y_{25}	552.032	x_{15}	445.326	$A_{20\text{-}36}$	17.2903	$A_{17\text{-}19}$	75.6	$A_{30\text{-}31}$	6.49	$A_{23\text{-}26}$	39.9	$A_{3\text{-}7}$	8.79
y_5	260.438	x_{27}	-85.107	y_{15}	48.998	$A_{2\text{-}19}$	4.3161	$A_{18\text{-}19}$	14.4	**277-bar (II)**		$A_{24\text{-}25}$	9.71	$A_{4\text{-}6}$	62
x_7	-64.180	y_{27}	599.788	x_{16}	518.860	$A_{3\text{-}19}$	23.7419	$A_{18\text{-}20}$	56.8	**(236543.28 lb)**		$A_{24\text{-}26}$	9.71	$A_{4\text{-}7}$	6.49
y_7	370.620	y_{29}	582.204	y_{16}	-0.055	$A_{4\text{-}19}$	3.1871	$A_{19\text{-}20}$	21.8	**in & in^2**		$A_{24\text{-}27}$	6.49	$A_{5\text{-}7}$	6.49
x_9	-53.706	$A_{1\text{-}3}$	0.5	y_{17}	37.942	$A_{3\text{-}20}$	3.1871	$A_{19\text{-}21}$	75.6	y_4	314.233	$A_{25\text{-}27}$	9.71	$A_{5\text{-}8}$	20
y_9	435.519	$A_{1\text{-}5}$	2.6	x_{18}	522.801	$A_{4\text{-}20}$	17.2903	$A_{20\text{-}21}$	15.8	y_7	485.359	$A_{25\text{-}28}$	56.8	$A_{5\text{-}9}$	4.99
x_{11}	-44.619	$A_{3\text{-}5}$	0.1	y_{18}	60.286	$A_{19\text{-}20}$	2.7935	**277-bar (I)**		y_{10}	617.425	$A_{26\text{-}29}$	42.7	$A_{6\text{-}10}$	7.61
y_{11}	513.943	$A_{3\text{-}7}$	0.1	$A_{1\text{-}2}$	3.131	$A_{1\text{-}2}$	6.9032	**(282032.88 lb)**		y_{13}	739.897	$A_{27\text{-}29}$	9.71	$A_{6\text{-}13}$	61.8
x_{13}	-53.559	$A_{3\text{-}8}$	0.5	$A_{2\text{-}3}$	1.333	$A_{1\text{-}3}$	27.7419	**in & in^2**		y_{16}	830.438	$A_{27\text{-}30}$	6.49	$A_{7\text{-}8}$	6.49
y_{13}	536.863	$A_{5\text{-}7}$	0.1	$A_{1\text{-}4}$	3.131	$A_{2\text{-}3}$	1.6129	y_{31}	748.714	y_{19}	899.228	$A_{28\text{-}30}$	9.71	$A_{7\text{-}9}$	5.57
x_{19}	-102.846	$A_{5\text{-}9}$	2.6	$A_{2\text{-}4}$	0.539	$A_{1\text{-}4}$	17.2903	$A_{1\text{-}2}$	21.8	y_{22}	950.765	$A_{28\text{-}31}$	56.8	$A_{8\text{-}11}$	24.1
y_{19}	628.453	$A_{7\text{-}9}$	0.5	$A_{2\text{-}5}$	1.333	$A_{3\text{-}4}$	4.1226	$A_{1\text{-}3}$	68.5	y_{25}	985.011	$A_{29\text{-}30}$	9.71	$A_{9\text{-}11}$	9.71
x_{21}	-10.378	$A_{9\text{-}11}$	1.6	$A_{2\text{-}6}$	1.081	**77-bar**		$A_{2\text{-}3}$	6.49	y_{28}	993.227	$A_{30\text{-}31}$	9.71	$A_{10\text{-}11}$	7.65
y_{21}	618.162	$A_{9\text{-}13}$	1.2	$A_{3\text{-}6}$	2.142	**(305963.97 lb)**		$A_{2\text{-}5}$	21.8	y_{31}	997.973	**277-bar (III)**		$A_{10\text{-}12}$	7.65
$A_{1\text{-}3}$	3.0	$A_{11\text{-}13}$	0.1	$A_{4\text{-}5}$	0.347	**in & in^2**		$A_{3\text{-}5}$	9.71	$A_{1\text{-}2}$	25.6	**(231943.31 lb)**		$A_{10\text{-}13}$	9.71
$A_{2\text{-}3}$	0.3	$A_{11\text{-}15}$	1.6	$A_{5\text{-}6}$	0.347	y_3	224.347	$A_{3\text{-}6}$	11.5	$A_{1\text{-}4}$	67.7	**in & in^2**		$A_{11\text{-}12}$	6.49
$A_{3\text{-}5}$	2.6	$A_{13\text{-}15}$	0.2	$A_{4\text{-}7}$	3.131	y_5	321.370	$A_{3\text{-}7}$	61.8	$A_{2\text{-}4}$	6.49	x_3	208.021	$A_{11\text{-}14}$	32.9
$A_{4\text{-}5}$	1.5	$A_{13\text{-}18}$	1.1	$A_{5\text{-}7}$	0.44	y_7	431.315	$A_{5\text{-}6}$	6.49	$A_{2\text{-}5}$	25.6	y_3	289.400	$A_{12\text{-}14}$	3.54
$A_{5\text{-}7}$	2.8	$A_{15\text{-}17}$	0.6	$A_{5\text{-}9}$	1.081	y_9	521.002	$A_{5\text{-}8}$	21.8	$A_{4\text{-}5}$	7.65	x_4	514.544	$A_{12\text{-}15}$	3.54
$A_{6\text{-}7}$	0.6	$A_{15\text{-}19}$	1.4	$A_{6\text{-}9}$	1.488	y_{11}	592.148	$A_{6\text{-}7}$	23.2	$A_{4\text{-}6}$	6.49	y_4	463.214	$A_{12\text{-}19}$	7.61
$A_{7\text{-}9}$	2.3	$A_{17\text{-}19}$	1.0	$A_{7\text{-}8}$	0.27	y_{13}	650.329	$A_{6\text{-}8}$	9.71	$A_{4\text{-}7}$	55.8	x_6	879.829	$A_{13\text{-}15}$	7.65
$A_{7\text{-}10}$	1.1	$A_{17\text{-}20}$	0.8	$A_{8\text{-}9}$	0.44	y_{15}	703.318	$A_{6\text{-}10}$	42.7	$A_{5\text{-}6}$	6.49	y_6	646.499	$A_{13\text{-}16}$	75.6
$A_{9\text{-}11}$	2.5	$A_{19\text{-}21}$	0.4	$A_{7\text{-}10}$	2.8	y_{17}	741.956	$A_{6\text{-}11}$	14.4	$A_{5\text{-}8}$	29.1	x_7	623.346	$A_{14\text{-}17}$	28.2
$A_{10\text{-}11}$	0.6	$A_{19\text{-}25}$	1.1	$A_{8\text{-}10}$	0.44	y_{19}	761.865	$A_{7\text{-}10}$	26.5	$A_{6\text{-}7}$	4.41	y_7	186.673	$A_{14\text{-}19}$	6.49
$A_{11\text{-}13}$	2.3	$A_{19\text{-}29}$	1.1	$A_{8\text{-}11}$	0.111	y_{21}	765.677	$A_{8\text{-}11}$	24.1	$A_{6\text{-}8}$	6.49	x_9	819.550	$A_{15\text{-}16}$	6.49
$A_{12\text{-}13}$	1.4	$A_{21\text{-}25}$	0.2	$A_{8\text{-}12}$	0.27	$A_{1\text{-}2}$	35.3	$A_{10\text{-}12}$	19.1	$A_{6\text{-}9}$	6.49	y_9	62.113	$A_{15\text{-}19}$	6.49
$A_{13\text{-}21}$	0.7	$A_{21\text{-}27}$	0.2	$A_{9\text{-}12}$	2.142	$A_{1\text{-}3}$	68.5	$A_{10\text{-}13}$	56.8	$A_{7\text{-}9}$	6.49	x_{10}	1107.381	$A_{16\text{-}18}$	83.3
$A_{13\text{-}15}$	1.6	$A_{21\text{-}29}$	0.2	$A_{11\text{-}12}$	0.111	$A_{2\text{-}3}$	3.54	$A_{11\text{-}12}$	9.71	$A_{7\text{-}10}$	56.8	y_{10}	433.965	$A_{17\text{-}19}$	3.54
$A_{19\text{-}21}$	0.9	$A_{23\text{-}25}$	1.1	$A_{10\text{-}13}$	2.697	$A_{2\text{-}4}$	35.3	$A_{11\text{-}14}$	31.2	$A_{8\text{-}11}$	32.9	x_{12}	1480.945	$A_{17\text{-}20}$	28.2
$A_{15\text{-}19}$	0.8	$A_{23\text{-}27}$	0.7	$A_{11\text{-}13}$	0.111	$A_{3\text{-}4}$	14.4	$A_{12\text{-}13}$	6.49	$A_{9\text{-}11}$	7.65	y_{12}	233.424	$A_{18\text{-}21}$	14.4
$A_{15\text{-}21}$	0.2	$A_{27\text{-}29}$	0.7	$A_{12\text{-}15}$	2.142	$A_{3\text{-}5}$	68.5	$A_{12\text{-}14}$	9.71	$A_{9\text{-}12}$	6.49	x_{13}	1227.996	$A_{18\text{-}25}$	83.3
$A_{17\text{-}19}$	0.9	**68-bar**		$A_{13\text{-}14}$	1.333	$A_{4\text{-}5}$	14.4	$A_{12\text{-}16}$	21.8	$A_{10\text{-}12}$	6.49	y_{13}	749.968	$A_{19\text{-}20}$	6.49
$A_{15\text{-}17}$	1.2	**(1166.0624 lb)**		$A_{14\text{-}15}$	0.954	$A_{4\text{-}6}$	46.7	$A_{12\text{-}17}$	15.6	$A_{10\text{-}13}$	56.8	x_{15}	1544.228	$A_{19\text{-}21}$	10
$A_{14\text{-}21}$	1.1	**in & in^2**		$A_{13\text{-}16}$	1.333	$A_{5\text{-}6}$	7.65	$A_{13\text{-}16}$	56.8	$A_{11\text{-}12}$	6.49	y_{15}	455.410	$A_{20\text{-}21}$	3.54
$A_{21\text{-}22}$	1.2	x_2	77.158	$A_{14\text{-}16}$	0.347	$A_{5\text{-}7}$	75.6	$A_{14\text{-}17}$	32.9	$A_{11\text{-}14}$	35.3	x_{16}	1633.329	$A_{20\text{-}23}$	32.9
110-bar		y_2	2.241	$A_{14\text{-}17}$	1.333	$A_{6\text{-}7}$	7.65	$A_{16\text{-}18}$	9.71	$A_{12\text{-}13}$	6.49	y_{16}	836.159	$A_{21\text{-}23}$	4.41
(1314.0468 lb)		x_4	102.478	$A_{14\text{-}18}$	0.539	$A_{6\text{-}8}$	50	$A_{16\text{-}19}$	67.7	$A_{12\text{-}14}$	9.71	x_{18}	2085.647	$A_{21\text{-}24}$	11.2
in & in^2		y_4	-63.299	$A_{15\text{-}18}$	1.174	$A_{7\text{-}8}$	9.71	$A_{17\text{-}18}$	17	$A_{12\text{-}15}$	6.49	y_{18}	921.111	$A_{23\text{-}24}$	3.54
x_1	-147.839	x_5	149.668	$A_{16\text{-}17}$	1.333	$A_{7\text{-}9}$	75.6	$A_{17\text{-}20}$	46.7	$A_{13\text{-}15}$	7.65	x_{19}	1790.757	$A_{23\text{-}26}$	32
x_3	-61.793	y_5	39.504	$A_{17\text{-}18}$	1.081	$A_{8\text{-}9}$	9.71	$A_{18\text{-}19}$	6.49	$A_{13\text{-}16}$	55.8	y_{19}	146.595	$A_{24\text{-}26}$	4.41
y_3	92.508	x_6	112.369	$A_{9\text{-}10}$	0.111	$A_{8\text{-}10}$	51.8	$A_{18\text{-}20}$	9.71	$A_{14\text{-}17}$	38.8	x_{21}	2243.269	$A_{24\text{-}28}$	6.49
x_5	-127.842	y_6	69.877	**224-bar**		$A_{9\text{-}10}$	13.3	$A_{18\text{-}22}$	21.8	$A_{15\text{-}17}$	9.71	y_{21}	179.840	$A_{24\text{-}29}$	8.79
y_5	139.089	x_7	206.289	**(3079.4455 Kg)**		$A_{9\text{-}11}$	75.6	$A_{18\text{-}23}$	14.4	$A_{15\text{-}18}$	6.49	x_{24}	2571.264	$A_{25\text{-}28}$	9.71
x_7	-24.589	y_7	-62.871	**cm & cm^2**		$A_{10\text{-}11}$	11.5	$A_{19\text{-}22}$	67.7	$A_{16\text{-}18}$	9.71	y_{24}	58.838	$A_{25\text{-}30}$	83.3
y_7	183.323	x_8	284.375	y_2	-150.800	$A_{10\text{-}12}$	55.8	$A_{20\text{-}23}$	50	$A_{16\text{-}19}$	56.8	x_{25}	2549.469	$A_{26\text{-}27}$	3.54
x_9	-108.653	y_8	-20.567	z_2	718.123	$A_{11\text{-}12}$	14.4	$A_{22\text{-}24}$	9.71	$A_{17\text{-}18}$	7.65	y_{25}	935.135	$A_{26\text{-}28}$	6.49
y_9	270.627	x_9	219.291	y_3	-46.344	$A_{11\text{-}13}$	75.6	$A_{22\text{-}25}$	75.6	$A_{17\text{-}20}$	38.8	x_{27}	2848.702	$A_{26\text{-}29}$	35.3
x_{11}	-88.025	y_9	54.045	x_3	-191.008	$A_{12\text{-}13}$	14.4	$A_{23\text{-}24}$	9.71	$A_{18\text{-}19}$	7.65	y_{27}	162.706	$A_{27\text{-}29}$	3.54
y_{11}	381.346	x_{10}	308.332	x_4	-172.365	$A_{12\text{-}14}$	55.8	$A_{23\text{-}26}$	51.8	$A_{18\text{-}20}$	9.71	x_{28}	2615.871	$A_{27\text{-}31}$	6.49
x_{13}	-39.385	y_{10}	-50.950	y_{19}	-44.058	$A_{13\text{-}14}$	14.4	$A_{24\text{-}25}$	6.49	$A_{18\text{-}21}$	6.49	y_{28}	378.151	$A_{30\text{-}31}$	7.65
y_{13}	362.847	x_{11}	372.474	x_{19}	-280.169	$A_{13\text{-}15}$	75.6	$A_{24\text{-}26}$	9.71	$A_{19\text{-}21}$	9.71	y_{30}	944.284		
x_{15}	-81.704	y_{11}	21.145	x_{20}	-322.412	$A_{14\text{-}15}$	14.4	$A_{24\text{-}28}$	14.4	$A_{19\text{-}22}$	55.8	y_{31}	499.294		